ICTP-IAEA Workshop on “The training in basic radiation materials science and its applications to radiation effects studies and development of advanced radiation-resistant materials”
Trieste, 10 – 21 November 2008

Radiation-induced Segregation

V.A. Pechenkin

SSC RF Institute of Physics & Power Engineering,

Obninsk, Russia

Outline

- **RIS of major, alloying and impurity elements in structural materials**
  - **Fe-Cr-Ni alloys and austenitic steels**
  - **Ferritic/martensitic steels**
  - **Reactor pressure vessel steels**
- **Component and point defect fluxes in alloys under irradiation**
  - **Mechanisms of RIS**
  - **Steady state component profiles near PD sinks**
- **Modeling of RIS**
- **Effect of RIS on radiation phenomena in alloys**
  - **precipitate stability**
  - **swelling**
  - **corrosion**
  - **embrittlement**
- **Experimental methods and data needed**

Introduction

Radiation-induced segregation (RIS) plays an important role in structure and phase changes in alloys under irradiation and can influence strongly on phase composition, swelling, corrosion and embrittlement of structural materials.

In particular, RIS of nickel near voids, precipitates and grain boundaries in Fe-Cr-Ni alloys can result in the formation of austenite regions in ferritic alloys or ferrite regions in austenitic alloys near point defect sinks.

A strong dependence of swelling on alloy composition can be understood as a result of segregation-induced bias caused by RIS near voids.

Study of RIS is of great importance for reactor performance.

RIS phenomenon

Redistribution (segregation) **of alloy components near point defect sinks: grain boundaries, sample surfaces, dislocations, voids, precipitates during irradiation of alloys with electrons, ions, neutrons.**

It was predicted by Anthony in 1971.

For the first time it was observed by Okamoto et al. in 1973 during irradiation of Fe-18Cr-8Ni-1Si in HVEM: segregation-induced strain field around the voids due to Si segregation with subsequent formation of $\gamma'(Ni_3Si)$ phase layer around voids.

Size of RIS regions

~ tens of nanometers

Temperature interval of RIS observation

$0{,}2 \div 0.6\ T_m$ – as for swelling

Fe-Cr-Ni alloys and austenitic steels

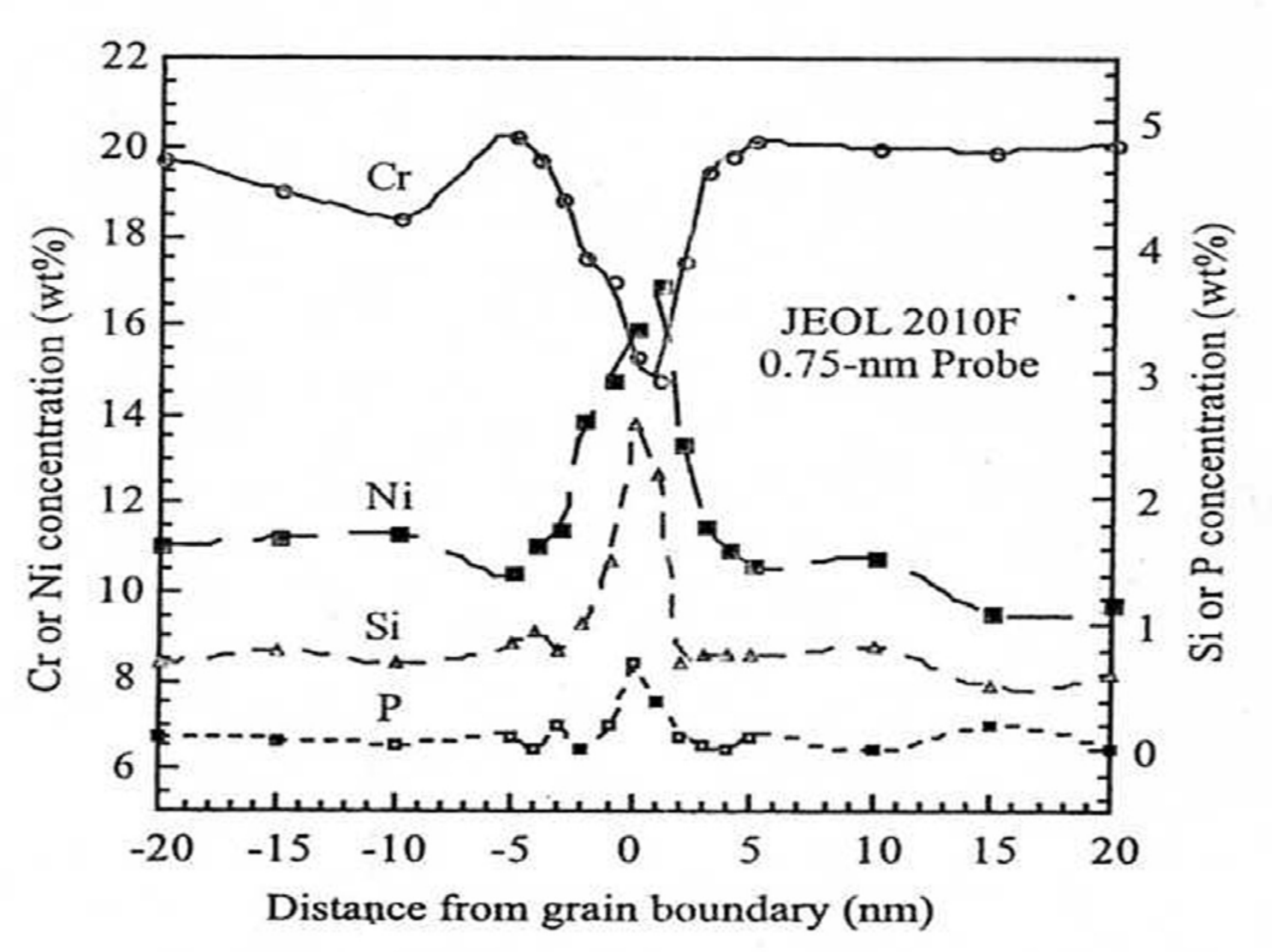

Radiation-induced segregation of Cr, Ni, Si and P at the grain boundary of a 300 series stainless steel irradiated in a light water reactor core to several dpa at~300^0C

(from Was, 2007)

Fe-Cr-Ni alloys and austenitic steels

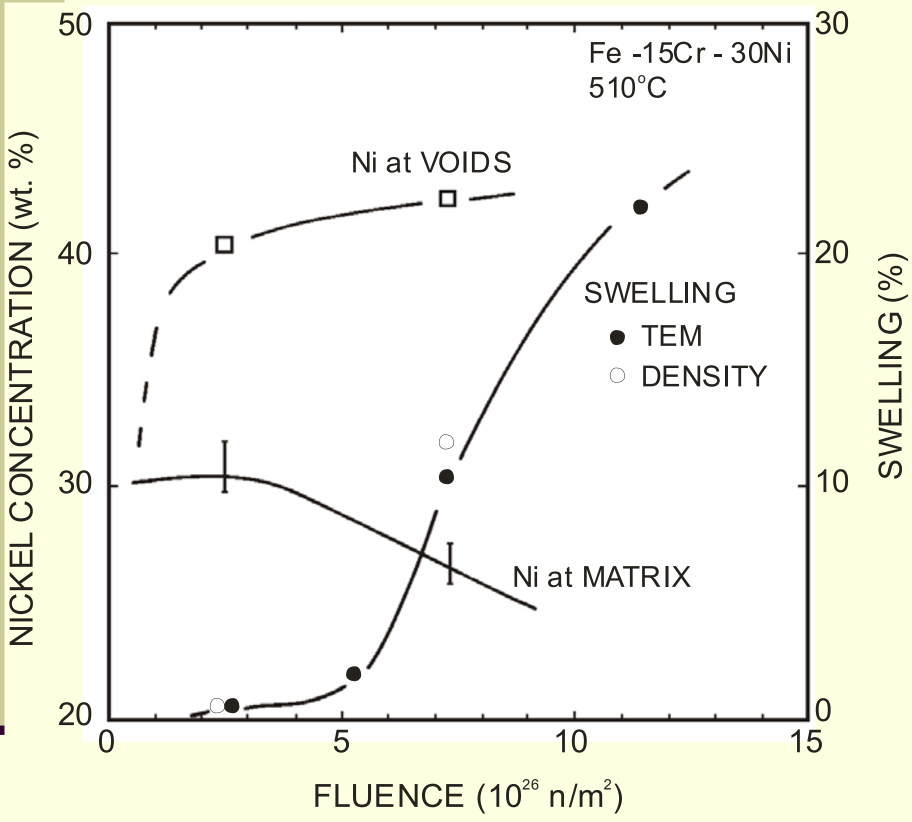

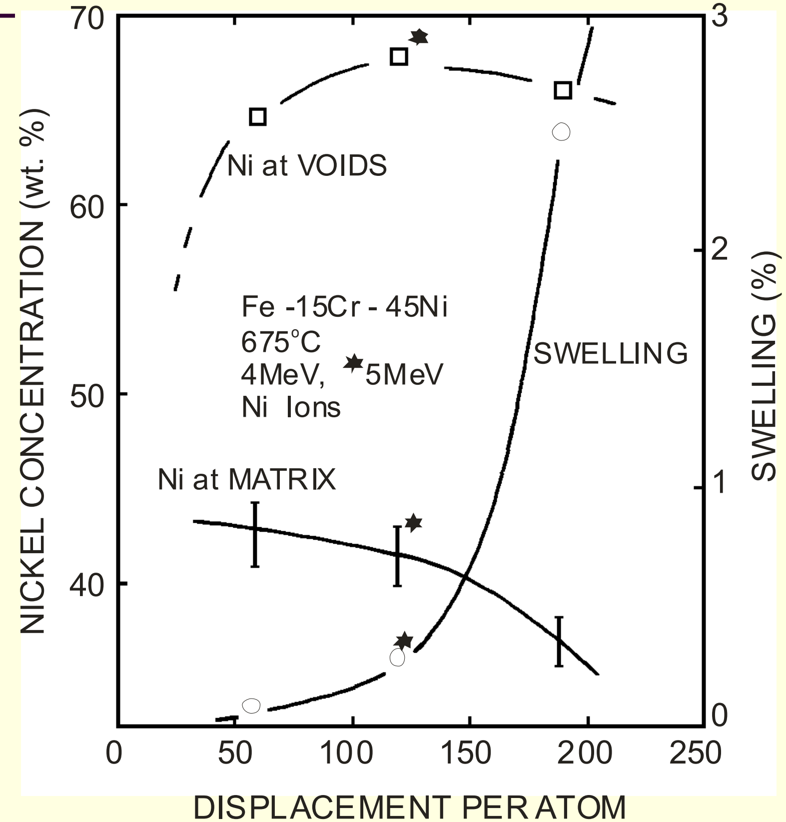

The dose dependence of swelling and nickel concentration at void surfaces and in the matrix of neutron irradiated Fe-15Cr-30Ni and Fe-15Cr-45Ni irradiated with 4 or 5 MeV Ni ions (Muroga et al., 1992)

Nimonic PE16

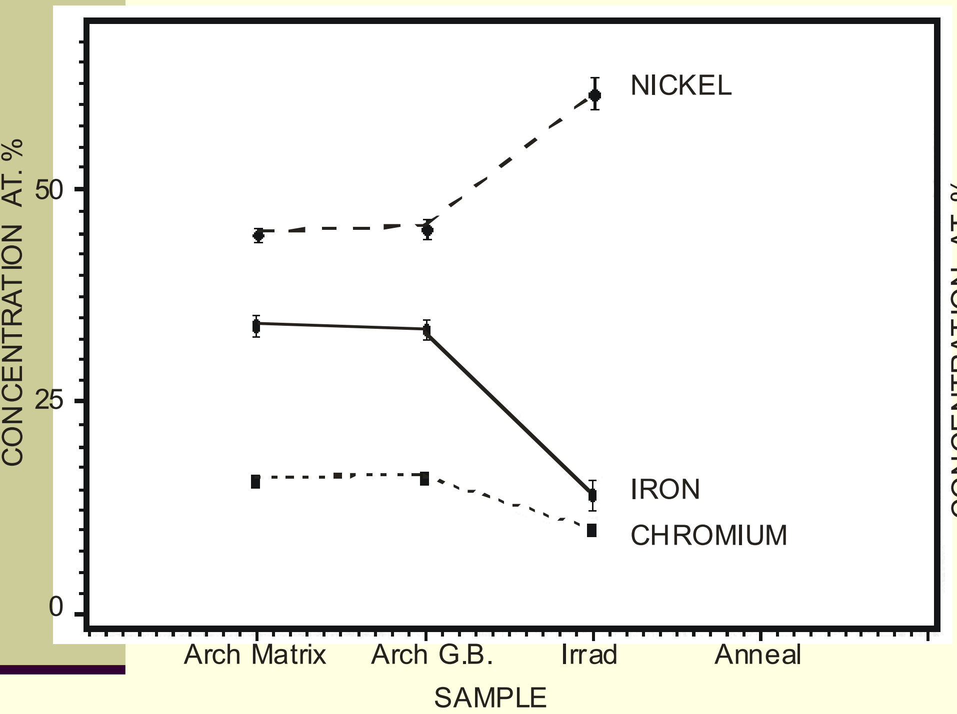

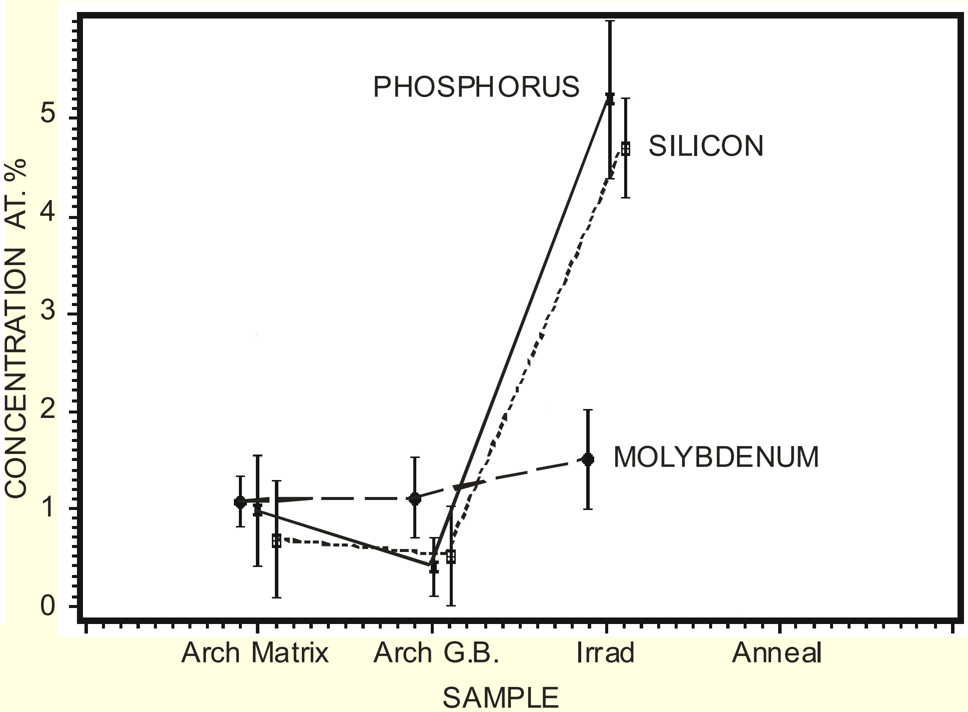

Composition of fracture surfaces for minor elements from archive and irradiated specimens of PE16, irradiated in AGR at 355^{0}C (Nettleship, 1992)

Ferritic/martensitic steels

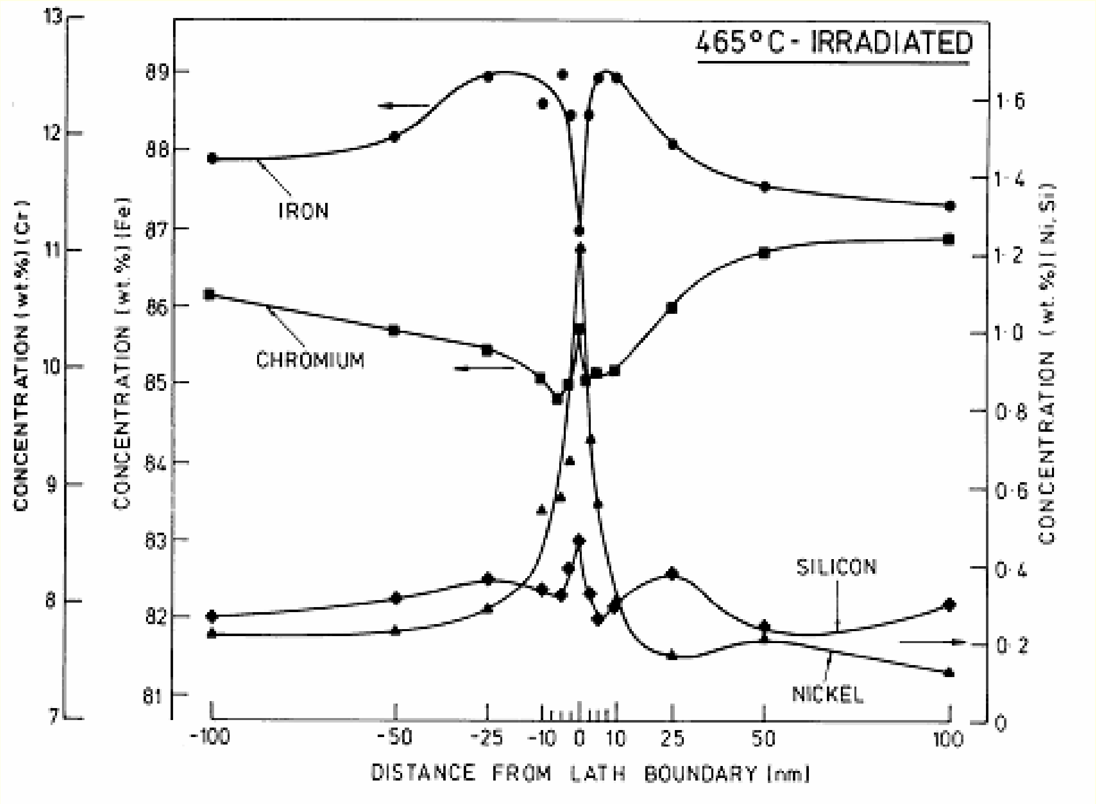

Typical concentration profiles for chromium, nickel, silicon and iron on either side of a lath boundary in a 12Cr-MoVNb (FV448) steel neutron-irradiated to 46 dpa (Morgan et al, 1992)

Reactor pressure vessel steels

a)

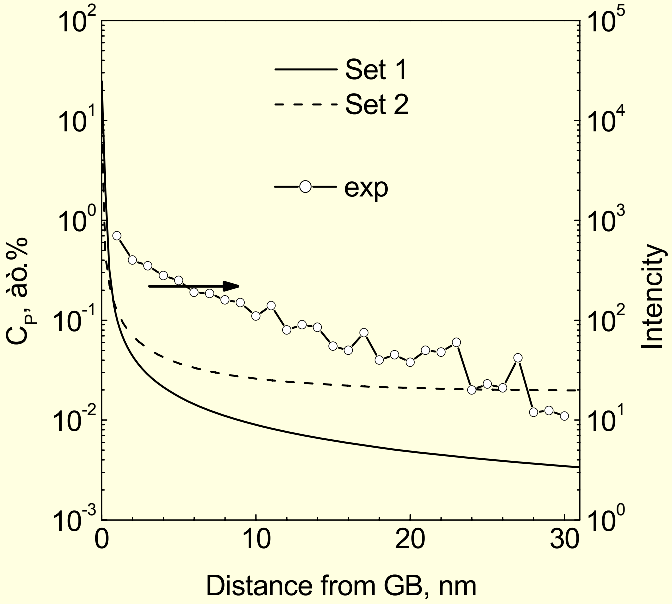

b)

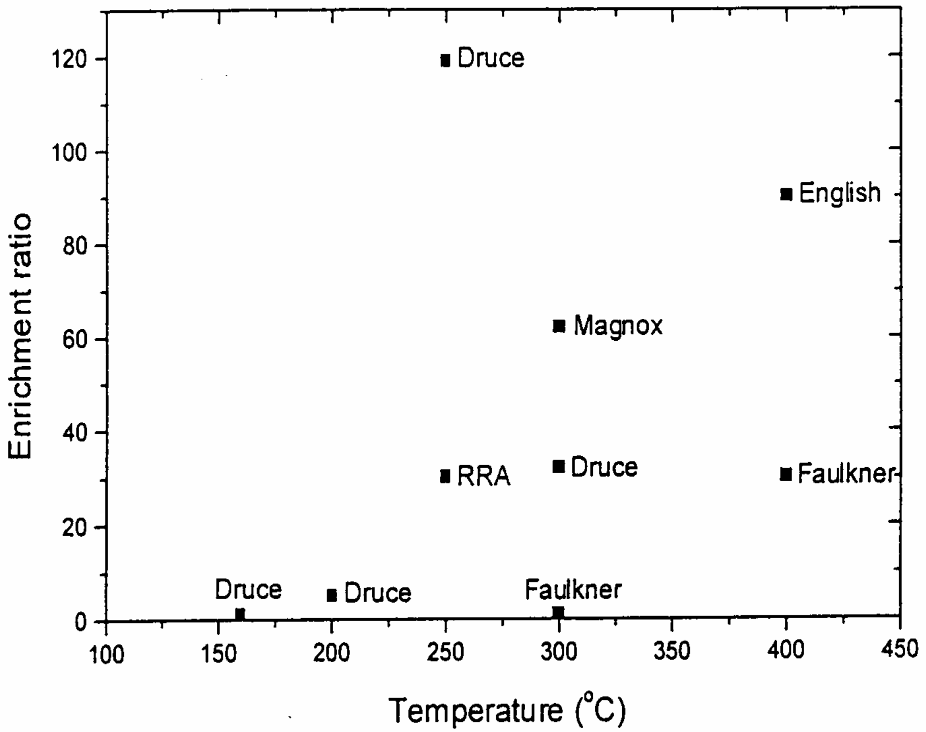

Experimental data on: a) P concentration profile near GB of irradiated VVER-440 base metal (Gurovich et al., 1997, SIMS results), b) P intergranular segregation in various RPVS (Faulkner et al., 1999)

RIS of major, alloying and impurity elements in structural materials

Austenitic steels:

enrichment of the matrix around sinks in Ni, Si, P, S
depletion in Fe, Cr, Mo, Ti, Mn

Ferritic/martensitic steels:

enrichment of the matrix around sinks in Ni, P, Si , Cr (?)
depletion in Fe

Reactor pressure vessel steels:

enrichment of the matrix around sinks in P, Si, Ni

Mechanisms of RIS

I. Inverse Kirkendall effect

(redistribution of elements in gradients of point defects due to a difference in the diffusivities of elements by vacancy or interstitial mechanism)

It is important for major components of austenitic (AS) and ferritic/martensitic steels (FMS)

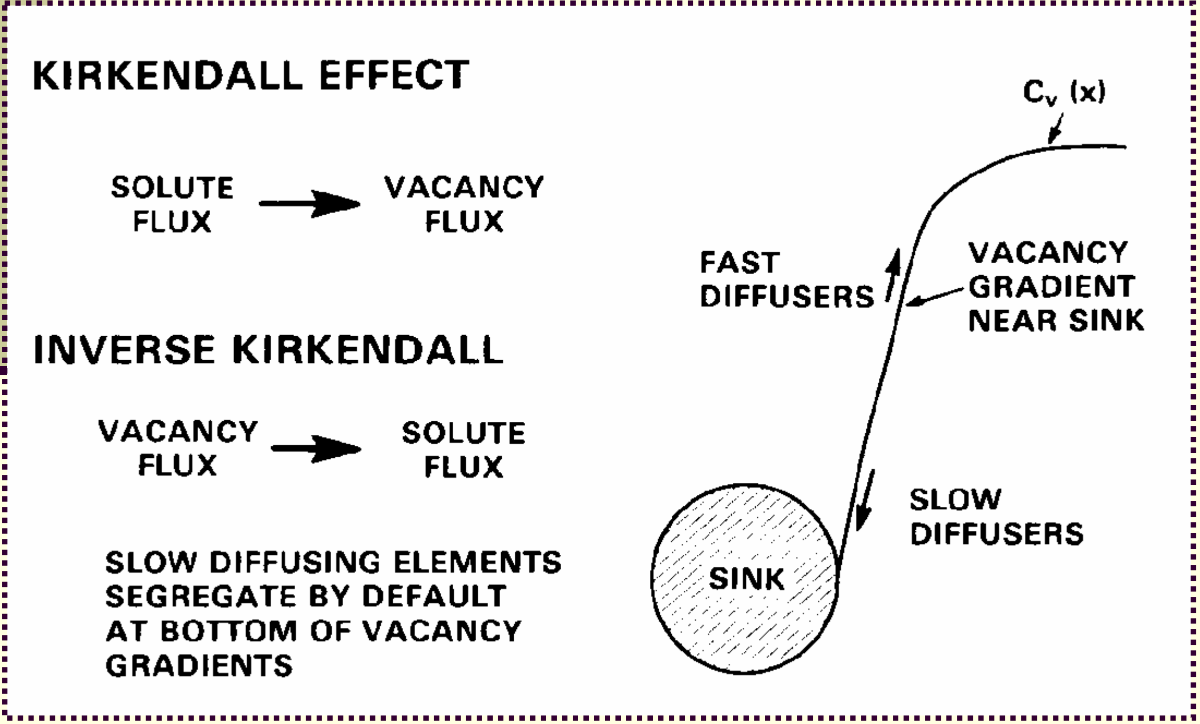

(Marwick et al., 1979)

Mechanisms of RIS

I. Inverse Kirkendall effect

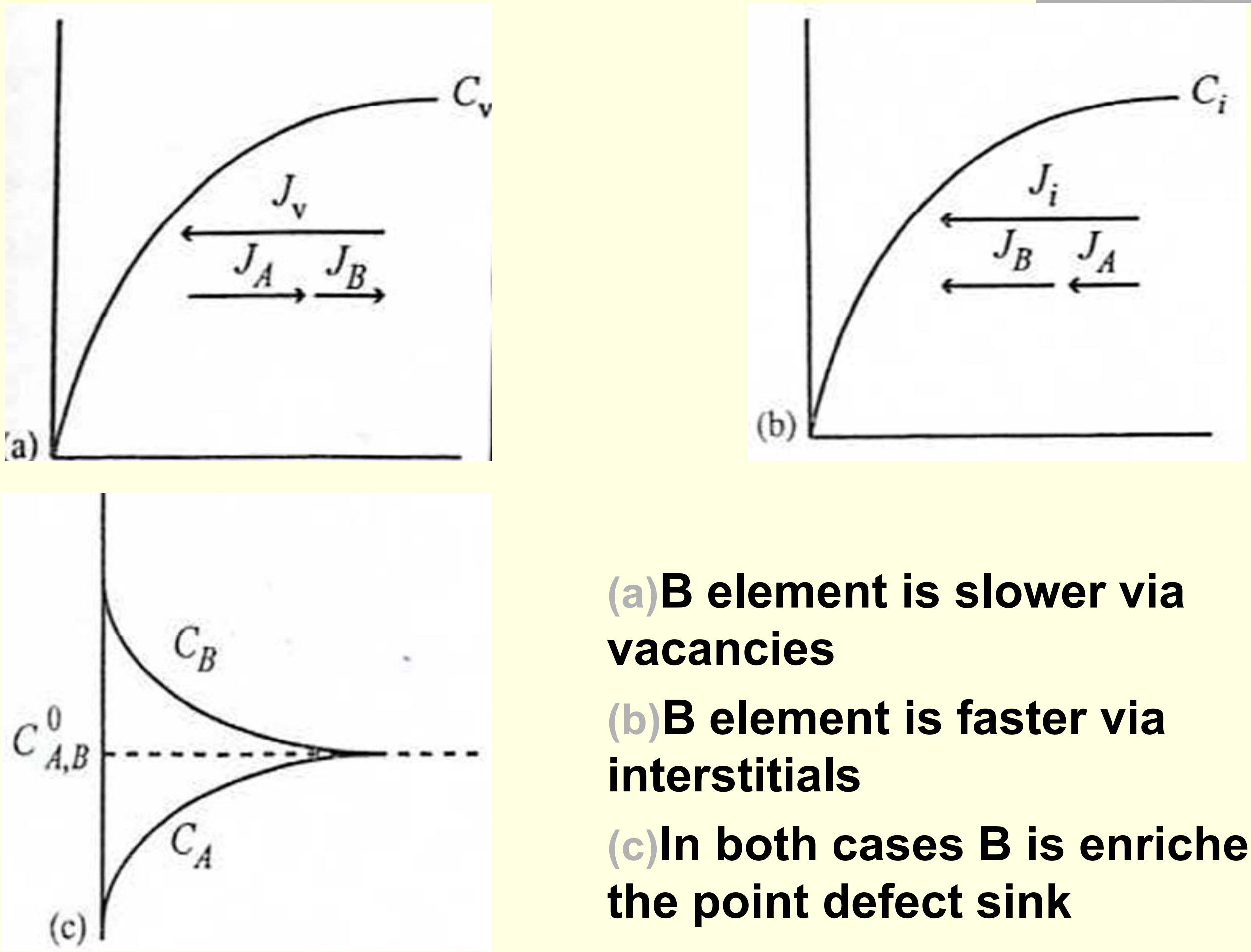

(a)**B element is slower via vacancies**

(b)**B element is faster via interstitials**

(c)**In both cases B is enriched near the point defect sink**

(from Was, 2007)

Mechanisms of RIS

II. Defect-solute complexes

(solute redistribution by vacancy-solute or interstitial-solute complexes due to a binding of some elements with point defects)

It is important for some solute and impurity elements especially for undersized ones: P, Si, S and others in AS and FMS and also for Fe, Cr in V-Fe, V-Cr, V-Fe-Ti, V-Cr-Ti alloys

Component and point defect fluxes in alloys under irradiation

The formalism of linear non-equilibrium thermodynamics represents the departures from thermodynamic equilibrium in terms of thermodynamic forces, X_j (defined in terms of gradients of chemical potential, temperature, etc), where j (=1,2,…) enumerates the distinct species or quantities whose flows may be measured (J_1, J_2, …). The phenomenological coefficients L_{ij} express the contribution of the force X_j, to the flux J_i, thus

$$J_i = \sum_j L_{ij} X_j$$

For component and point defect fluxes in *concentrated alloys* (Lidiard, Darken, Manning et al.) it follows after neglecting the correlation effects

$$J_k = \frac{D_k C_k}{kT} X_k + \frac{C_k}{kT} (d_{ki} C_i X_i - d_{kv} C_v X_v)$$

$$J_i = \frac{C_i}{kT} \sum_k d_{ki} C_k (X_k + X_i) \quad , \qquad J_v = -\frac{C_v}{kT} \sum_k d_{kv} C_k (X_k + X_v)$$

Component and point defect fluxes in alloys under irradiation

Diffusion coefficients of components, vacancies and interstitials are

$$D_k = d_{ki}C_i + d_{kv}C_v, \quad D_v = \sum_j d_{jv}C_j \qquad D_i = \sum_j d_{ji}C_j$$

At constant temperature thermodynamic forces include external forces and gradients of chemical potentials (α = v,i)

$$X_j = F_j - \nabla\mu_j, \quad \mu_k = \mu_{ko}(T,P) + kTln(\gamma_k C_k),$$

$$\mu_\alpha = kT\ln(C_\alpha / C_{\alpha e}), C_{\alpha e} = \exp(-G_\alpha^f / kT)$$

Component and point defect fluxes in alloys under irradiation

If external forces and the dependence of PD formation and migration energies on alloy composition are not important than the simplest form of component and point defect fluxes can be obtained that accounts for the main reason of RIS – the difference in component diffusivities

$$J_k = -D_k \alpha_k \nabla C_k + C_k [(d_{kv} \nabla C_v - d_{ki} \nabla C_i)],$$

$$J_v = -D_v \nabla C_v + C_v \sum_k d_{kv} \alpha_k \nabla C_k$$

$$J_i = -D_i \nabla C_i - C_i \sum_k d_{ki} \alpha_k \nabla C_k$$

where $\alpha_k = 1 + \dfrac{\partial \ln \gamma_k}{\partial \ln C_k}$ **are the thermodynamic factors**

Steady state component profiles near PD sinks

Here we will consider a model where the sinks of each kind k (k = f, v, d и g for a foil, void, dislocation and grain boundary) are arranged in an ordered fashion with the outer radius

$$R_f = L/2, \quad R_d = \left(\frac{1}{\pi \rho_d}\right)^{1/2}, \quad R_v = \left(\frac{3}{4\pi N_v}\right)^{1/3},$$

where L **–foil width,** ρ_d **–dislocation density,** N_v **–void concentration**

Steady state component profiles can be obtained from the conditions (binary alloy):

$J_A=0$ and $J_n=J_{n0}$ (n=v,i)

Concentrated binary alloy

$$\frac{C_A(x)}{[1-C_A(x)]^{\nu}} = C \cdot C_{v0}(x)^{\theta},$$

Where

$$\nu = \frac{1}{\lambda_i \lambda_v} \frac{d_{Bv}/D_{v0} + d_{Bi}/D_{i0}}{d_{Av}/D_{v0} + d_{Ai}/D_{i0}}, \quad \theta = \frac{\lambda_i - \lambda_v}{\alpha \lambda_i \lambda_v [d_{Av}/D_{v0} + d_{Ai}/D_{i0}]}, \quad \lambda_n = d_{Bn}/d_{An}$$

$C_{v0}(x)$ – the profile of vacancy concentration under irradiation near the sink in nonsegregated alloy (Pechenkin, Epov, 1992)

The shape of A component profile (its enrichment or depletion at a sink) depends on the relation of component diffusivities by vacancy and interstitial mechanisms defined by Θ

Concentrated ternary alloy

$$C_a = \frac{1}{1 + C_1\left[\frac{C_a}{\varphi}\right]^{\xi} + C_2\left[\frac{C_a}{\varphi}\right]^{(1-\beta)\xi}}, \qquad C_b = C_2 C_a\left[\frac{C_a}{\varphi}\right]^{(1-\beta)\xi},$$

$$\beta = \frac{d_{bv}d_{ci} - d_{cv}d_{bi}}{d_{av}d_{ai} - d_{cv}d_{ai}}\,\frac{d_{av}d_{i0} + d_{ai}d_{v0}}{d_{bv}d_{i0} + d_{bi}d_{v0}}, \varepsilon = \frac{d_{ci}}{d_{i0}}\,\frac{d_{av}d_{i0} + d_{ai}d_{v0}}{d_{av}d_{ci} - d_{ai}d_{cv}}.$$

where $\xi=1/(\varepsilon-1)$ **and** $\varphi= C_v^{1/a}$

The shape of component profiles (its enrichment or depletion on a sink) depends on the relation of component diffusivities by vacancy and interstitial mechanisms defined by β and ε

Multicomponent alloys

After some simplifications one can find

$$C_k = \frac{C_{k0}\left(\dfrac{C_{v0}}{< C_{v0} >}\right)^{g_{kN}^{0}}}{\sum_{j}^{n} C_{j0}\left(\dfrac{C_{v0}}{< C_{v0} >}\right)^{g_{kN}^{0}}}$$

where $g_{kN}^{0} \sim d_{kv} d_{Ni} - d_{ki} d_{Nv}$,

the index "*N*" relates to one of the main alloy components

Fe-Cr-Ni alloys and austenitic steels

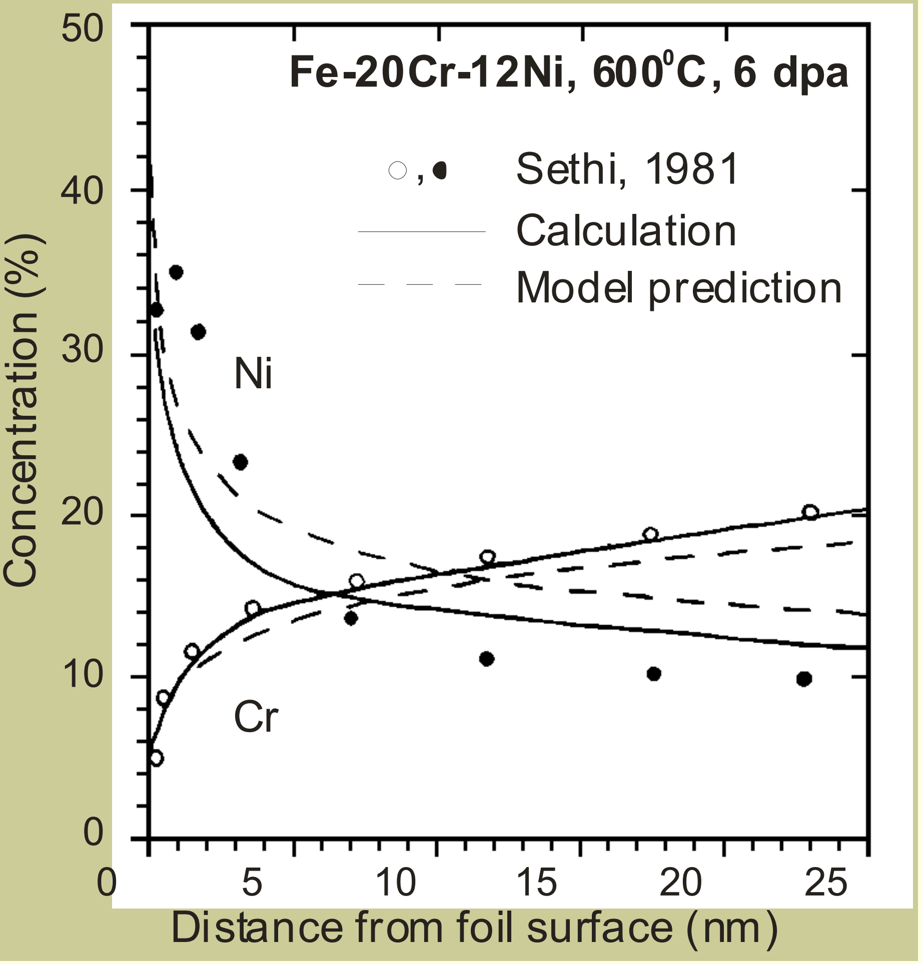

Results of RIS numerical calculations (Perks et al.,1986) and analytical model predictions (Pechenkin, Epov, 1992) fitted to the data by Sethi and Okamoto on component segregation near a sample surface of Fe-20Cr-12Ni alloy irradiated with 3 MeV Ni ions at a damage rate of 2×10^{-3} dpa/s

Ferritic/martensitic steels

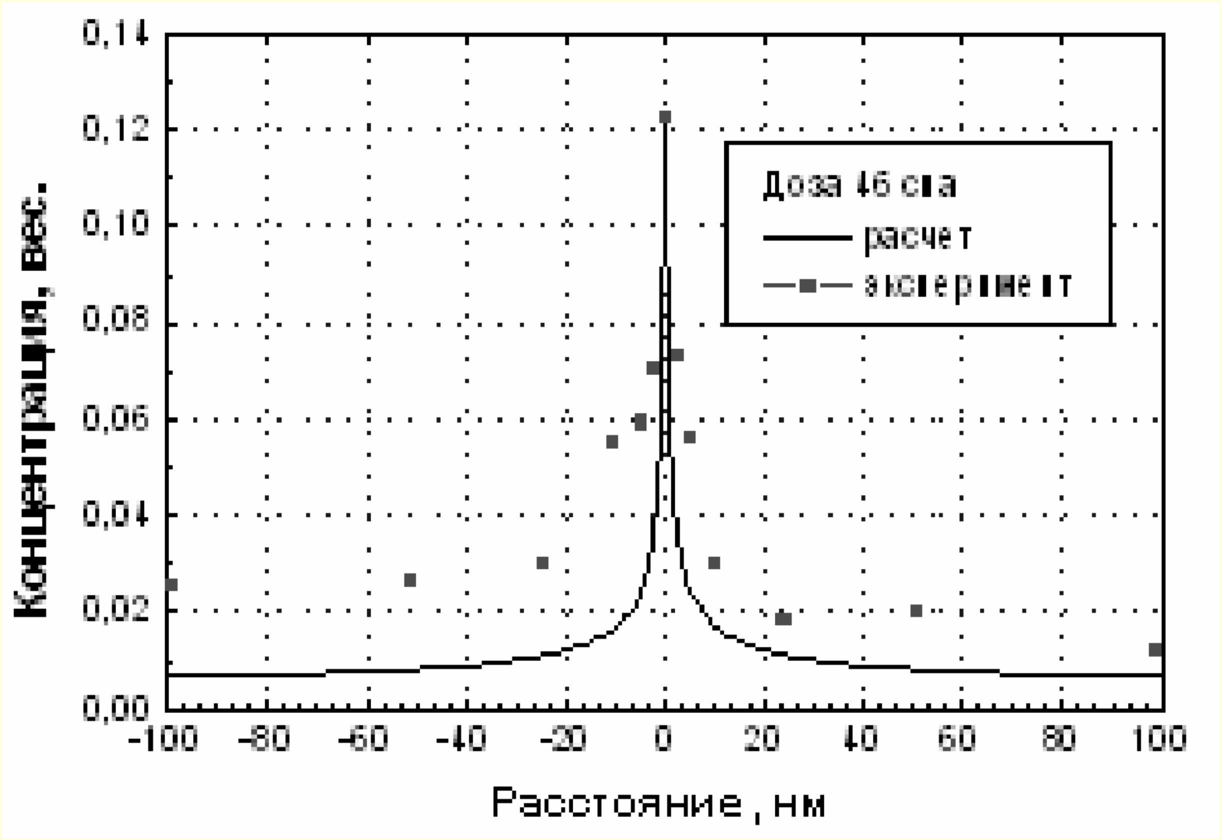

Concentration profiles for nickel on either side of a lath boundary in a 12Cr-MoVNb (FV448) steel neutron-irradiated in PFR to 46 dpa at 288 °C (Morgan et al, 1992) together with calculated ones (Epov et al., 1997)

Fe-Cr-Ni alloys and austenitic steels

Fe -15Cr -25Ni -0.1P 593°C, 14.3 dpa

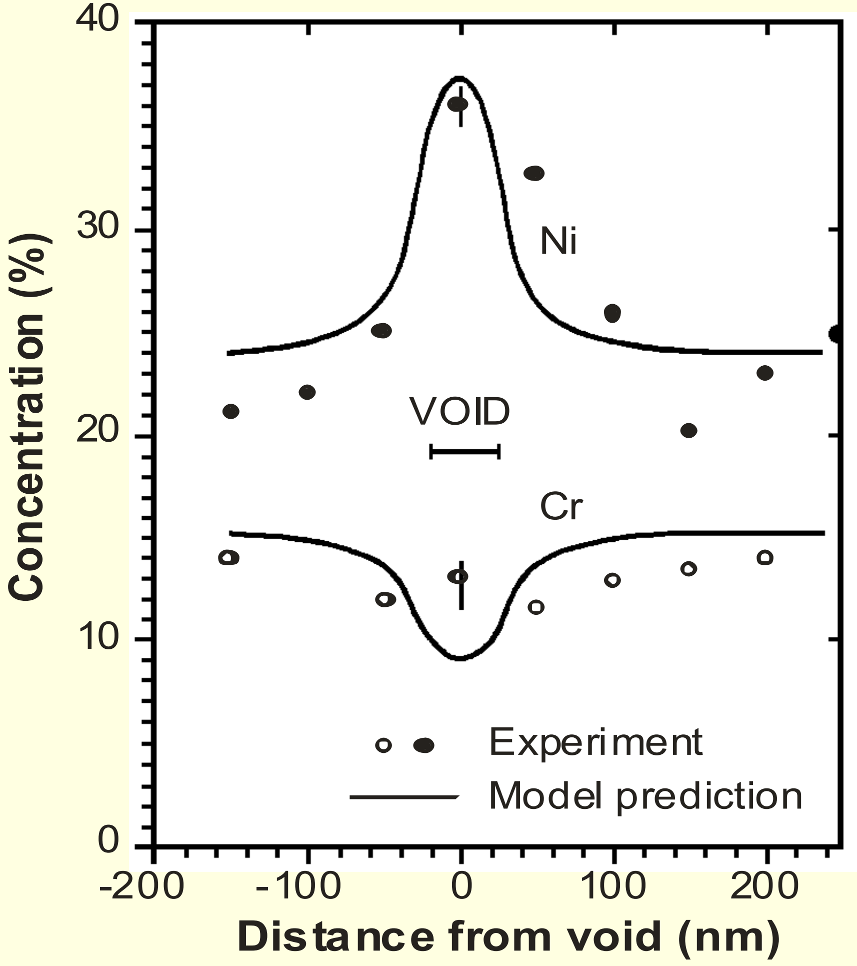

Comparison of a compositional traverse of the matrix including a void (Muroga et al., 1989) with model prediction (Pechenkin, Epov, 1992)

Modeling of radiation – induced segregation

- Diffusion equations for component C_m and point defect (PD) C_n concentrations in ternary alloys (ordered sinks):

$$\frac{\partial C_n}{\partial t} = -\nabla J_n + \varepsilon K - \mu_R C_v C_i, \ (n = v, i),$$

$$\frac{\partial C_m}{\partial t} = -\nabla J_m, \ (m = a, b, c),$$

where K is the PD generation rate, ε is the cascade efficiency, μ_R is the recombination coefficient

Modeling of radiation – induced segregation

- Diffusion equations for component C_m and point defect (PD) C_n concentrations in ternary alloys (lossy medium):

$$\frac{\partial C_k}{\partial t} = -\nabla J_k$$

$$\frac{\partial C_v}{\partial t} = -\nabla J_v + \varepsilon \cdot K - \mu_R D_i C_i C_v - k_i^2 D_i C_i$$

$$\frac{\partial C_i}{\partial t} = -\nabla J_i + \varepsilon \cdot K - \mu_R D_i C_i C_v - k_v^2 D_v (C_v - C_v^e)$$

Modeling of radiation – induced segregation

Perks model

Segregation driven by preferential interaction of alloying elements with the vacancy flux (inverse Kirkendall)

$d_{Av} \neq d_{Bv} \neq d_{Cv}$

$d_{Ai} = d_{Bi} = d_{Ci}$

Modified Inverse Kirkendall (MIK) model for RIS in Fe-Cr-Ni alloys

(Allen, Was)

calculate migration energies based on local composition(Grandjean et al. Ni-Cu)

Approximation of interatomic “bonds”,

Only vacancy mechanism of RIS

Modeling of radiation – induced segregation

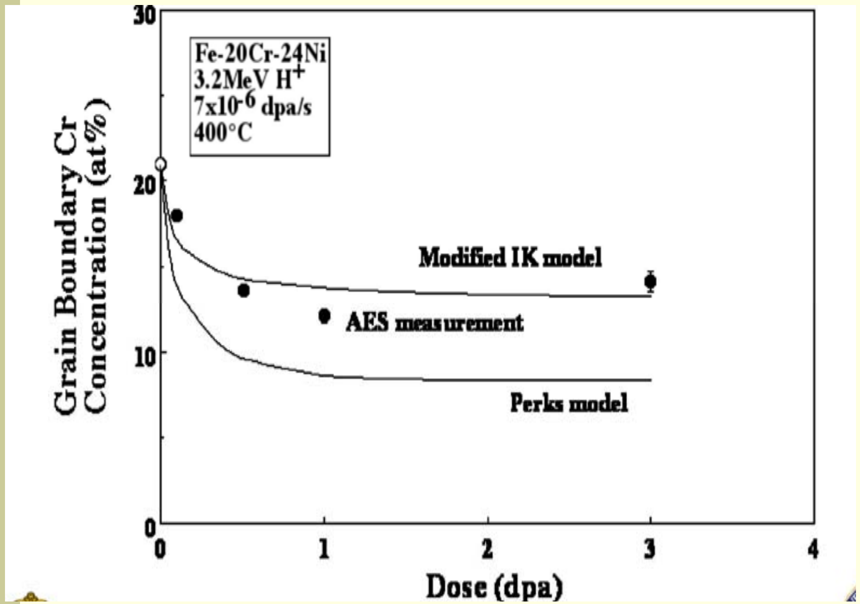

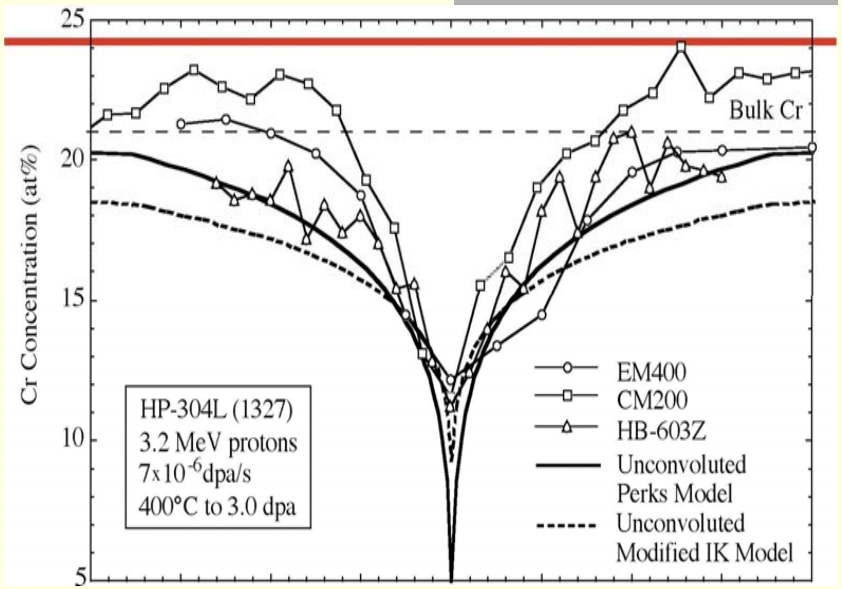

MIK better fits with experimental data on RIS in Fe-Cr-Ni alloys

Modeling of radiation – induced segregation

— Radiation-induced segregation of undersized minor elements can significantly influence on phase stability and swelling in alloys.

A ternary substitutional alloy is considered, in which the minor component A is undersized and forms tightly bound mixed dumbbells with B and C component atoms.

At sufficiently high temperatures the thermal equilibrium is assumed for the nonrandom occupation of interstitials by A-, B- and C- atoms:

$$\frac{C_i^A}{C_i} = \frac{\xi \cdot C_A}{\xi \cdot C_A + C_B + C_C}, \quad \frac{C_i^B}{C_i} = \frac{C_B}{\xi \cdot C_A + C_B + C_C}, \quad \frac{C_i^C}{C_i} = \frac{C_C}{\xi \cdot C_A + C_B + C_C},$$

where C_i and C_m are the interstitial and alloy component (m=A,B,C) concentrations respectively, $\xi=\exp(E_b/kT)$, E_b the binding energy of mixed dumbbells AB and AC

Modeling of radiation – induced segregation

$$J_i = -\nabla \frac{d_{ai}\xi C_a + d_{bi} C_b + d_{ci} C_c}{1 + (\xi - 1) C_a} C_i ,$$

$$J_v = (d_{av} - d_{cv}) C_v \nabla C_a + (d_{bv} - d_{cv}) C_v \nabla C_b - D_v \nabla C_v ,$$

$$J_a = -d_{ai} \nabla \frac{\xi C_i C_a}{1 + (\xi - 1) C_a} - d_{av} C_v \nabla C_a + d_{av} C_a \nabla C_v ,$$

$$J_b = -d_{bi} \nabla \frac{C_i C_b}{1 + (\xi - 1) C_a} - d_{bv} C_v \nabla C_b + d_{bv} C_b \nabla C_v ,$$

Modeling of radiation – induced segregation

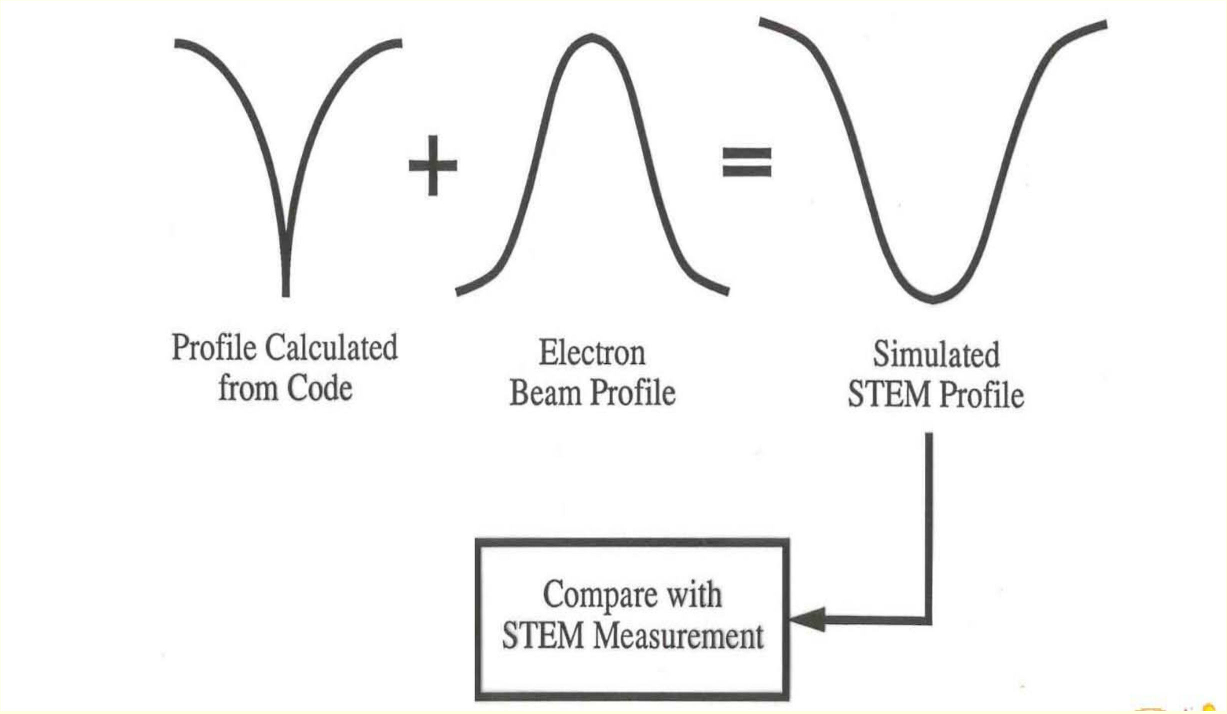

For a correct comparison of calculated alloy component profiles near sinks with experimental data, it is necessary to take into account the resolution of an experimental method (the radius R of the Gaussian electron beam intensity distribution used for microanalysis)

Fe-Cr-Ni alloys and austenitic steels

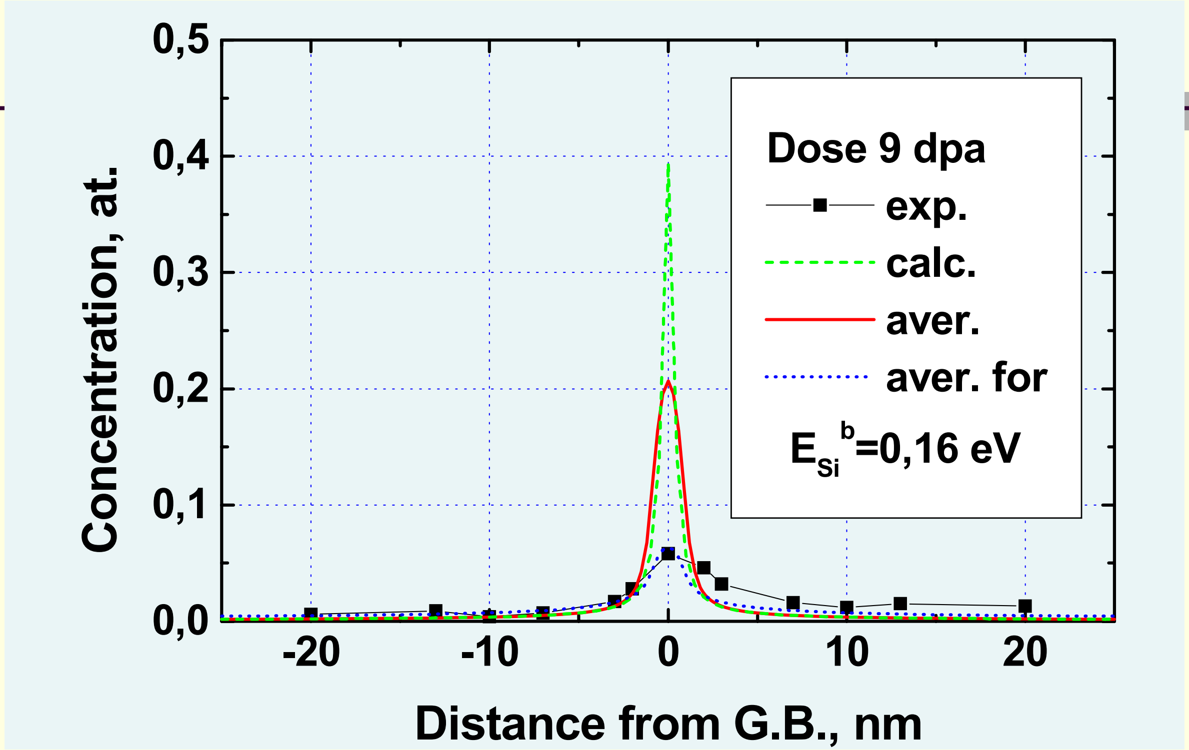

Comparison of as-calculated (E_{Si}^{b}=0.23 eV) and averaged (E_{Si}^{b}=0.23 and 0.16 eV) Si profiles across a GB (Pechenkin, Stepanov, 1999) with experimental data (Kenik et al., 1991)

Fe-Cr-Ni alloys and austenitic steels

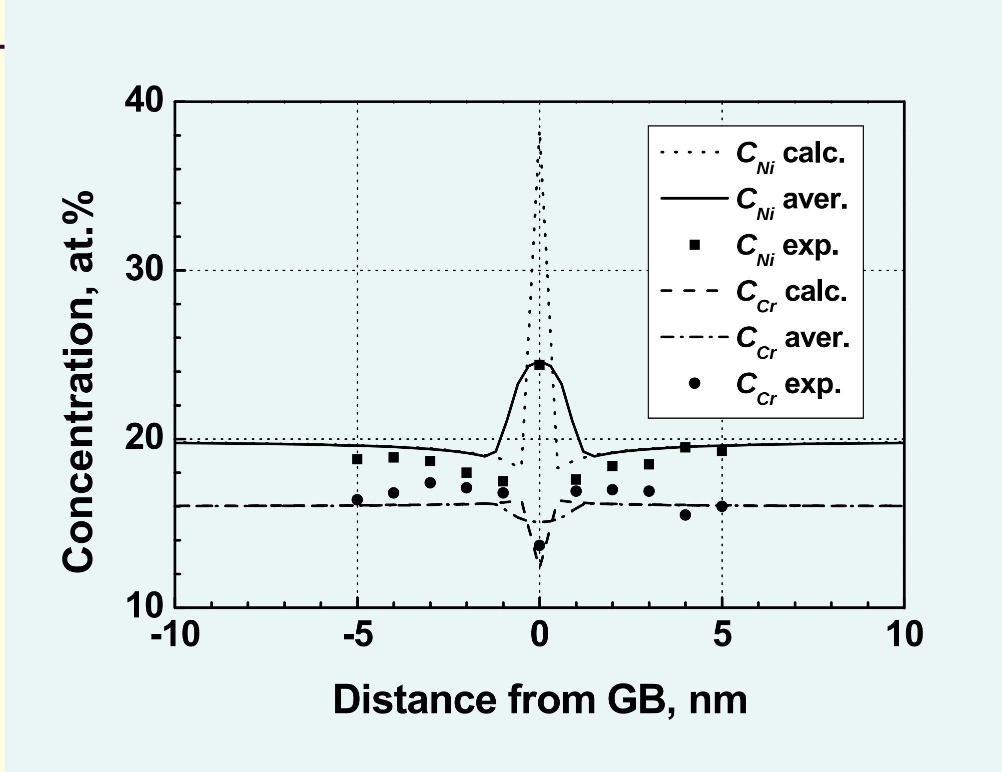

- *Calculated (Stepanov, Pechenkin, 2002) and experimental (Watanabe et al., 1997) Ni and Cr component profiles near GB in Fe-16Cr-20Ni alloy electron irradiated to 7.2 dpa at 323 K*

Under low-temperature electron irradiation (20-50°C) the RIS of alloy components near GB of initially homogeneous Fe-16Cr-20Ni alloy is observed, that can not be explained only by the vacancy mechanism of diffusion.

The best agreement between the experimental and calculated profiles was achieved at the binding energy of Ni atoms with interstitials of 0.03 eV.

Fe-Cr-Ni alloys

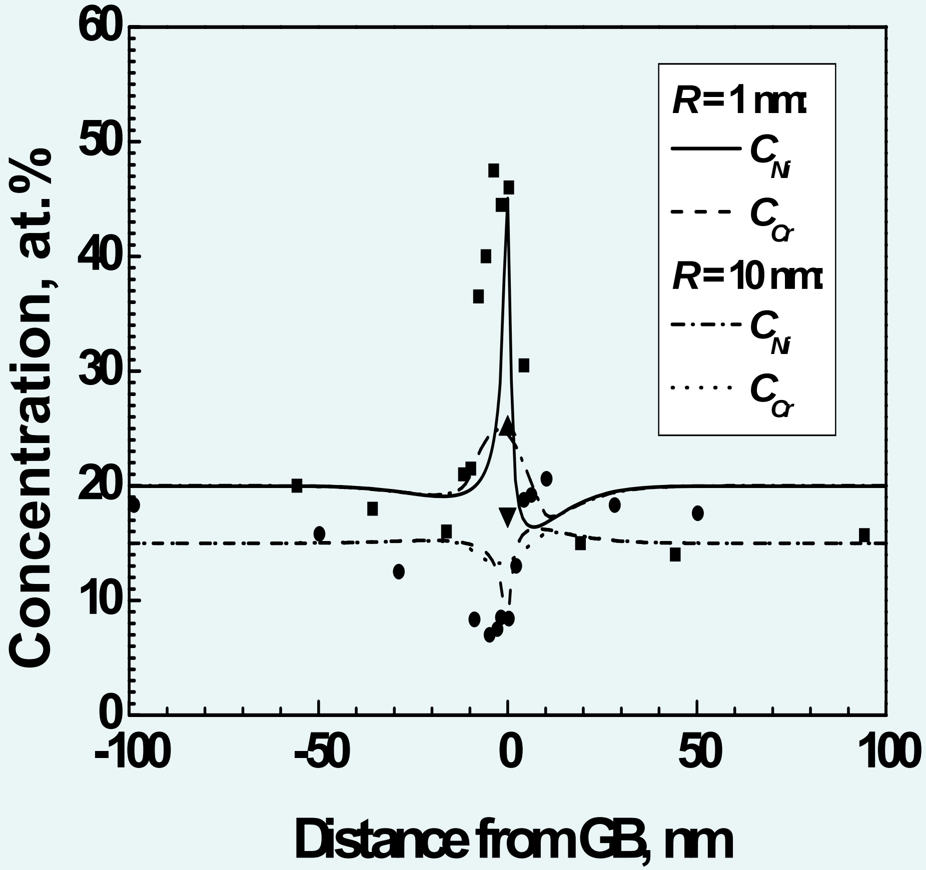

Experimental , Watanabe, 1996 (■ – Ni, ● – Cr, R=1 nm; ▲ – Ni, ▼ – Cr, R=10 nm) and calculated (Stepanov, Pechenkin, 2004) profiles of Ni and Cr concentrations near a moving GB at the dose of 3 dpa, $K=1\times10^{-3}$ dpa/s, T_{irr}=573 K

An account of the experimental method resolution is important

Fe-Cr-Ni alloys

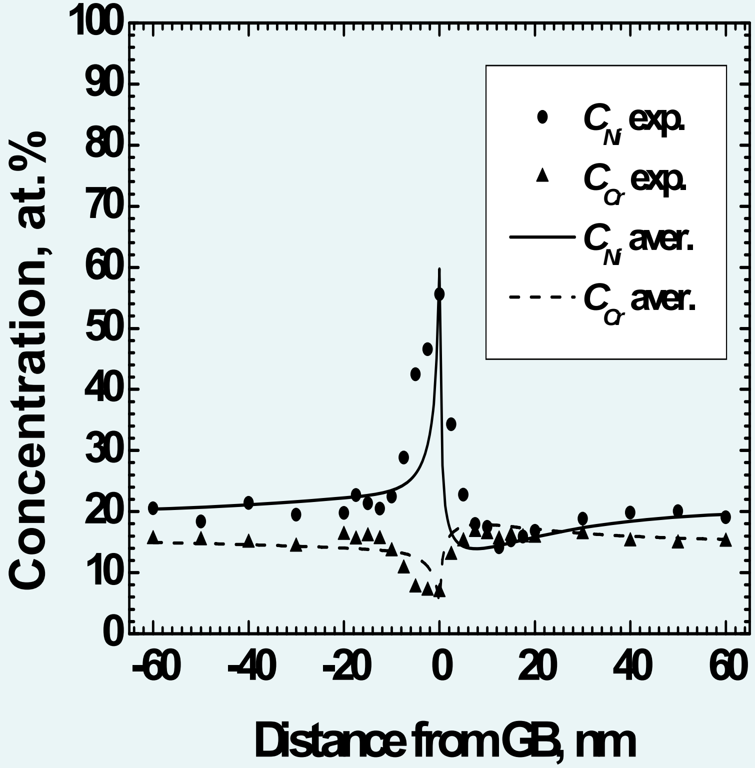

Experimental , Watanabe, 1996, and calculated (Stepanov, Pechenkin, 2004) profiles of Ni and Cr concentrations near a moving GB at the dose of 14.4 dpa, $K=4\times10^{-3}$ dpa/s, Tirr=623 K.

Fe-Cr-Ni alloys

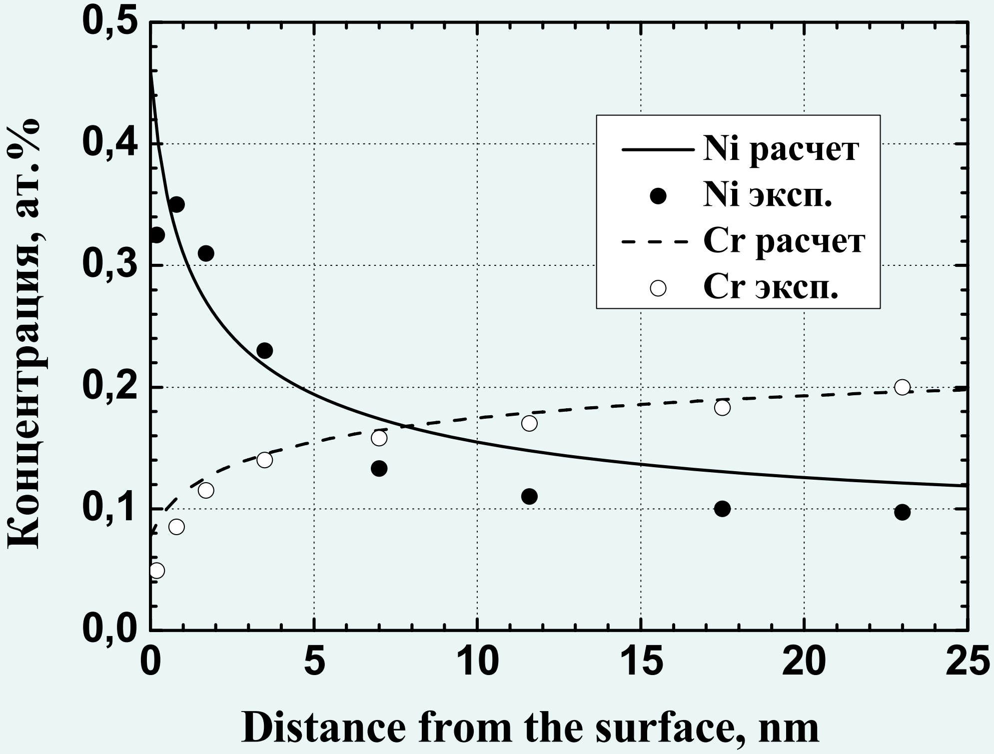

Results of RIS numerical calculations (Stepanov, Pechenkin, 2007) fitted to the data by Sethi and Okamoto on component segregation near a sample surface of Fe-20Cr-12Ni alloy irradiated with 3 MeV Ni ions at a damage rate of 2×10^{-3} dpa/s

Reactor pressure vessel steels

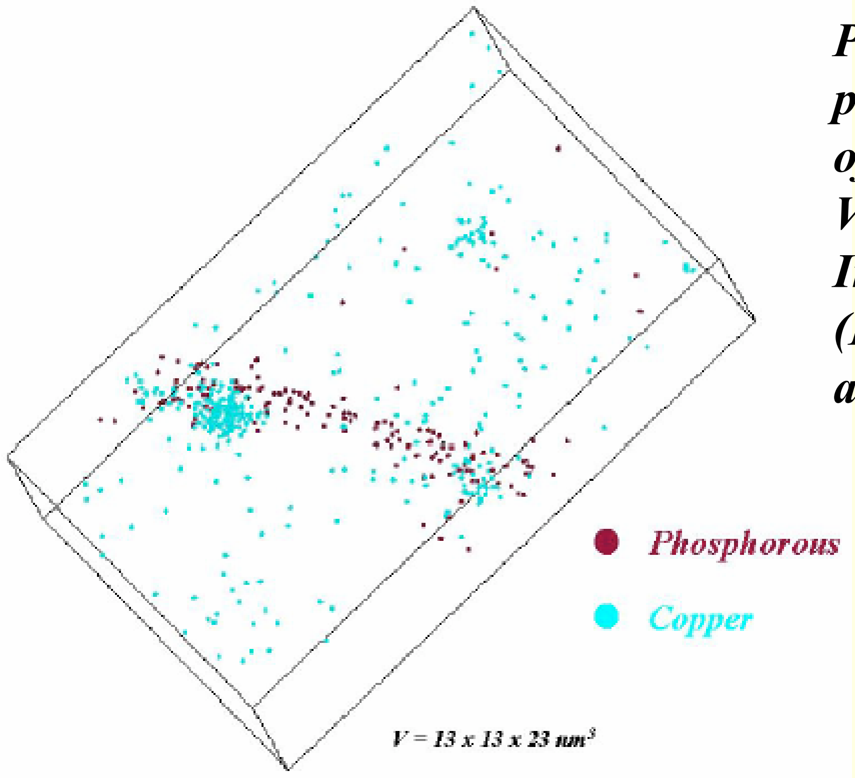

Phosphorus segregation and a copper-enriched precipitate on a dislocation in the base metal of the inside layer of the Novovoronezh Unit 2 VVER 440 vessel. Only Cu and P atoms are shown. Irradiation conditions are a fluence of 6.5×10^{23} n m^{-2} (E>0.5 MeV) (flux: 12×10^{14} n m^{-2}s^{-1}) and at a temperature of 275°C (Miller, Pareige, 2001)

Solute concentrations at the core of dislocations in atomic percent (P concentration agree with the calculations by Stepanov et al., 2004).

Fe	Cu	Mn	Ni	Si	Cr	P	V	C
84.3±2.9	0.9±0.8	4.5±1.6	1.9±1.1	3.0±1.3	1.9±1.1	3.4±1.4	-	-
83.7±2.2	2.3±0.9	3.3±1.1	1.3±0.7	2.2±0.9	2.2±0.9	2.4±0.9	2.0±0.8	0.6±0.5

Phosphorus Segregation at Dislocations

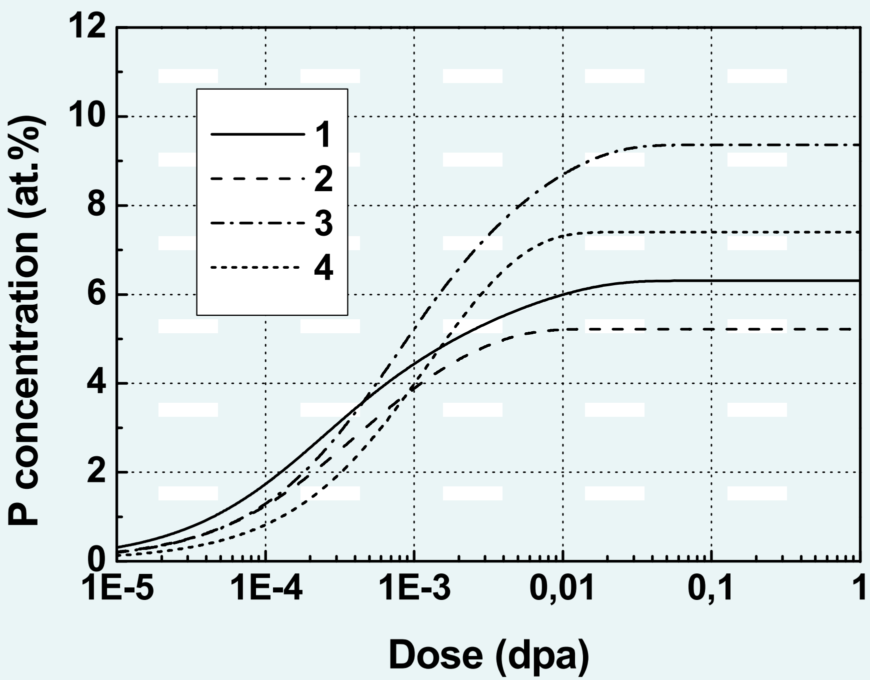

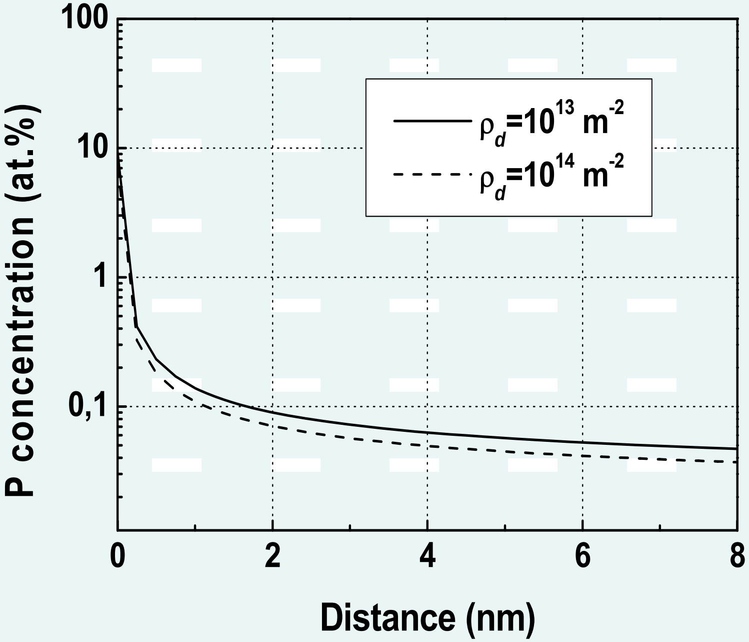

Dose dependence of P-concentration at the dislocation core for different dislocation core radii and dislocation densities: 1, 2 – R_d=0.5 nm, 3, 4 – R_d=1.0 nm for ρ_d=10^{13} and 10^{14} m-2, respectively in Fe-0.026P (at.%)

Calculated profiles of P near a dislocation core (Rd=1 nm) at the dose of 0.1 dpa for two dislocation densities

(Stepanov et al, 2004)

Phosphorus Segregation at Precipitates

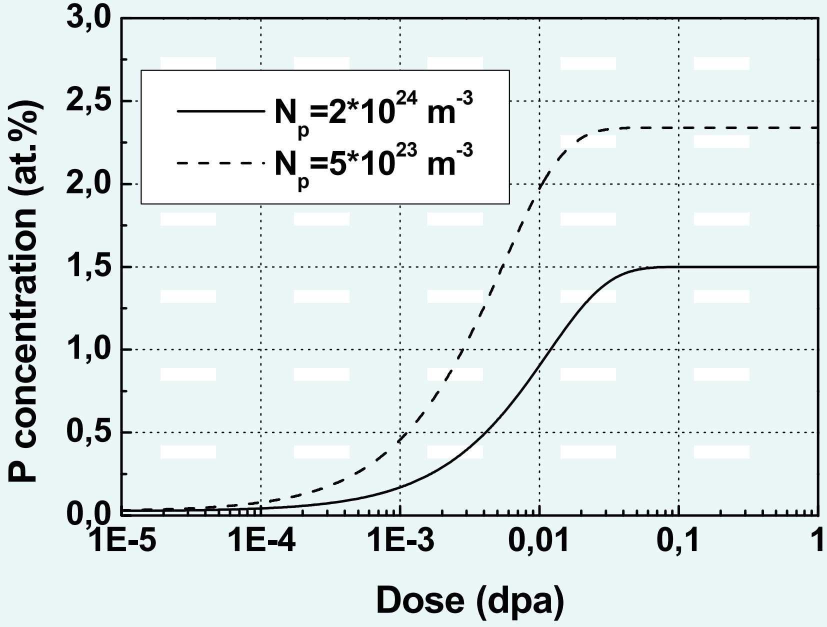

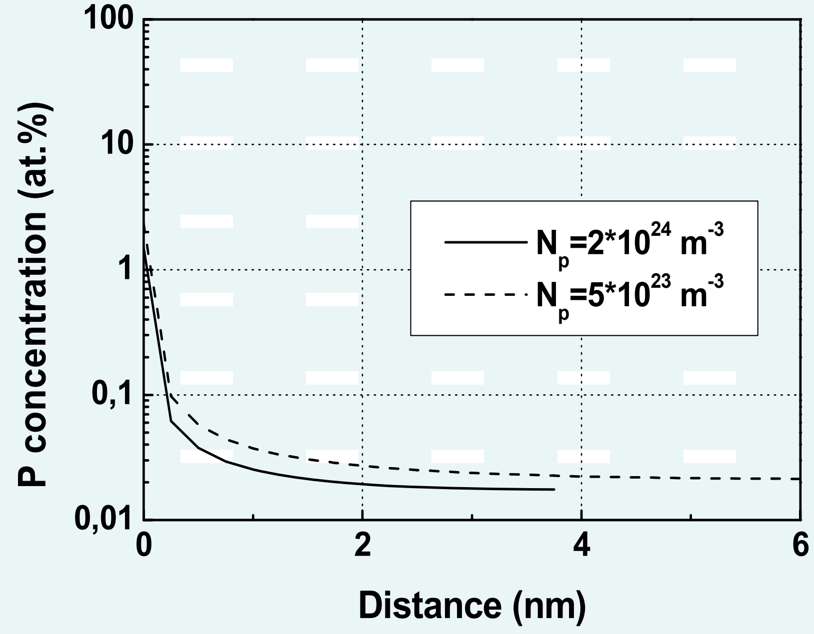

P-concentration on the surface of a spherical precipitate versus dose for two precipitate number densities (mean precipitate diameters are equal to 2.5 and 3 nm, respectively)

Calculated profiles of P near the precipitate surface at 0.1 dpa and different precipitate concentrations

Phosphorus Segregation at Grain Boundaries

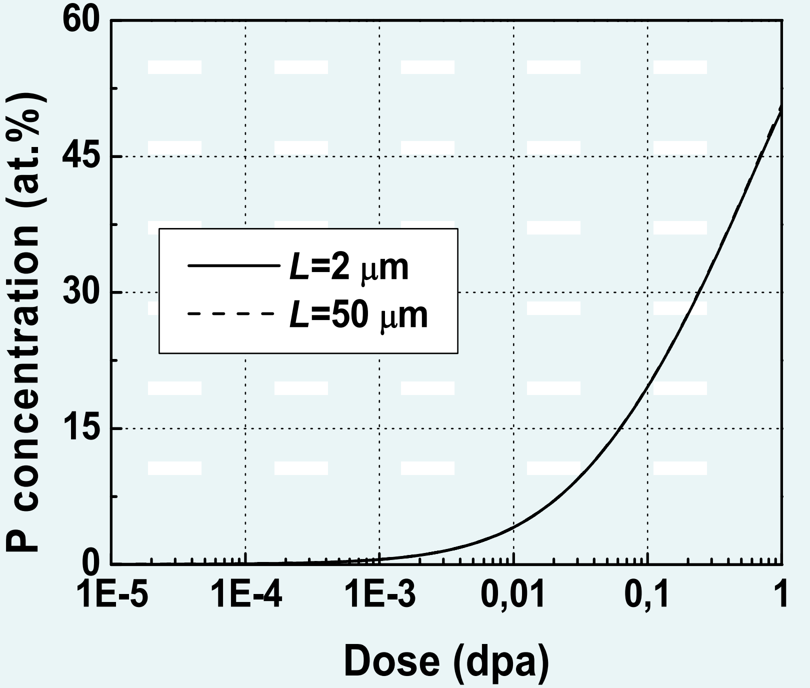

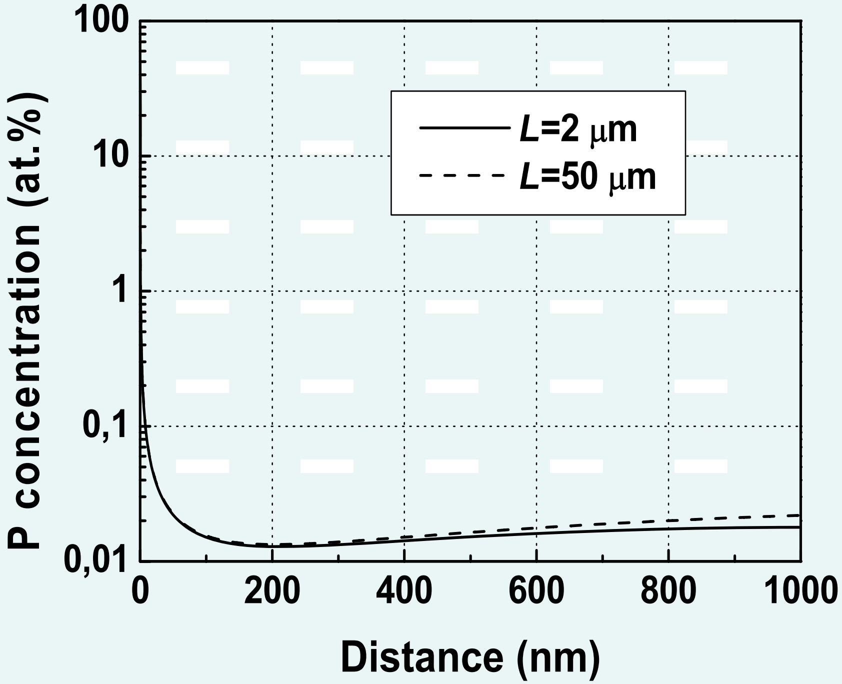

Dose dependence of P-concentration at a grain boundary for two grain sizes

Calculated profiles of P near a grain boundary at the dose of 1 dpa

Effect of dose rate

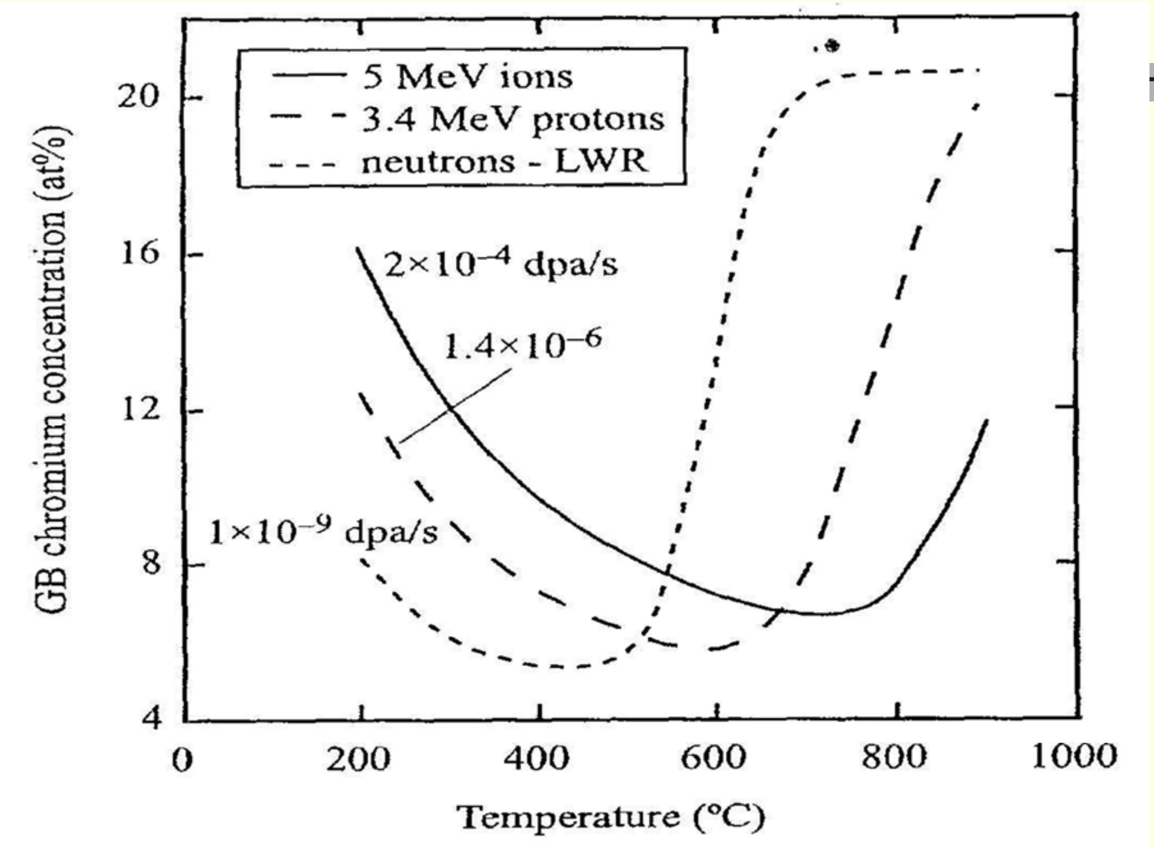

Dependence of grain boundary chromium concentration on temperature for particles with various dose rates (from Was, 2007)

Effect of dose rate

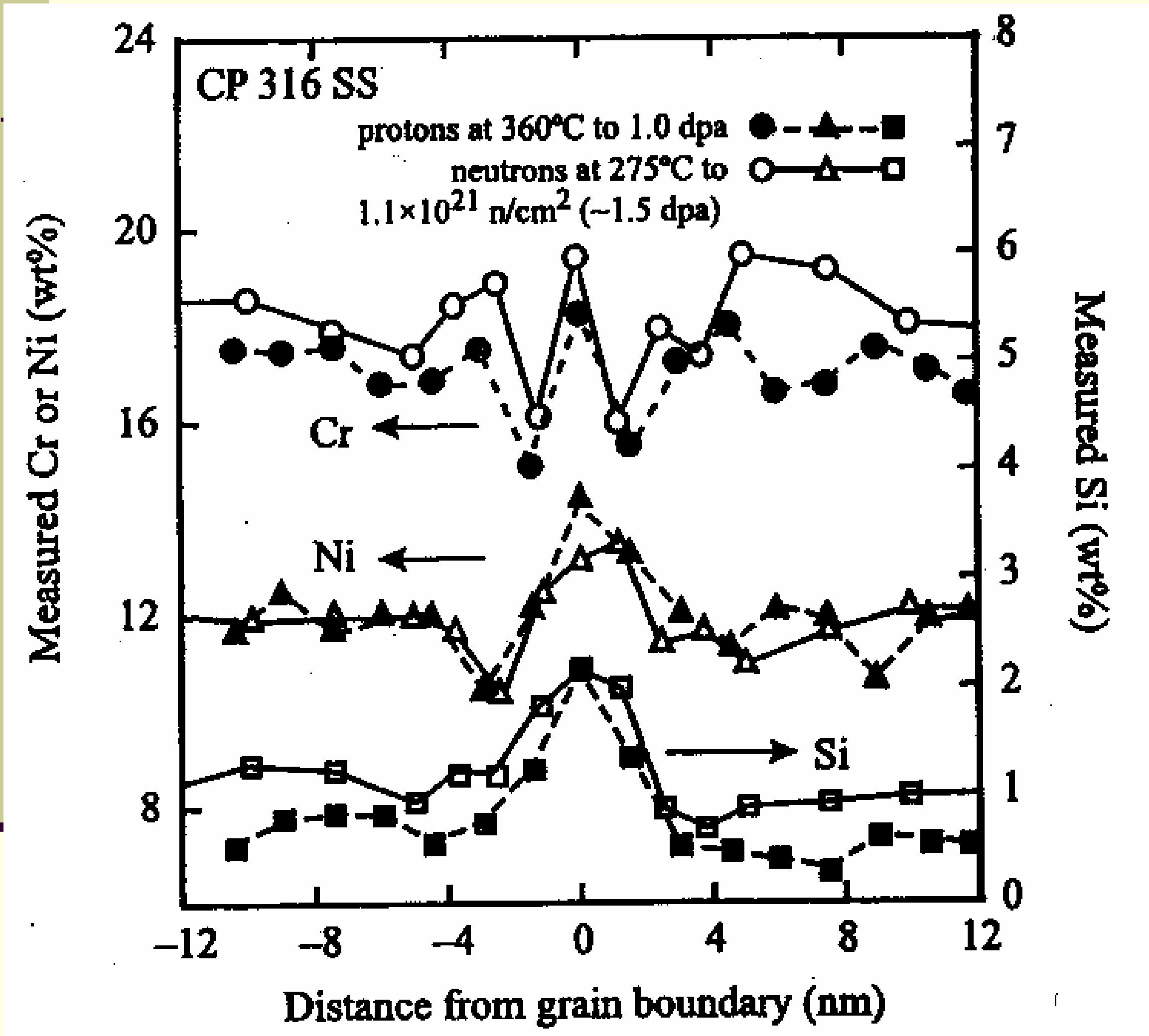

Comparison of grain boundary segregation of Cr, Ni and Si commercial purity 316 stainless steel following irradiation with either protons or neutrons to similar doses

(from Was, 2007)

Effect of dose rate

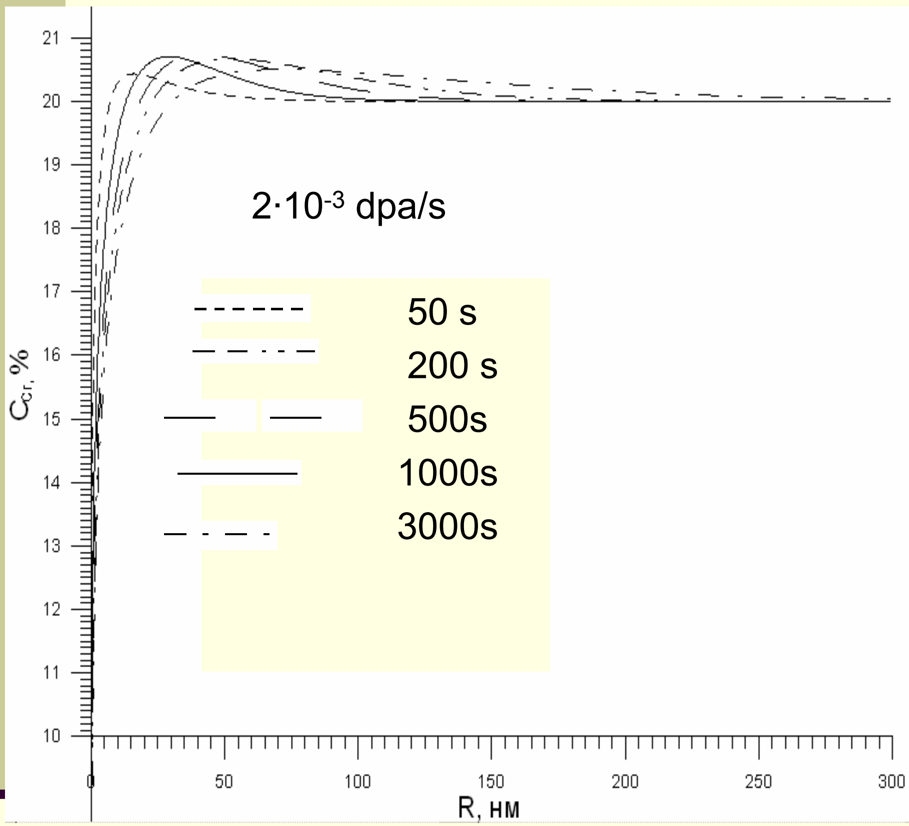

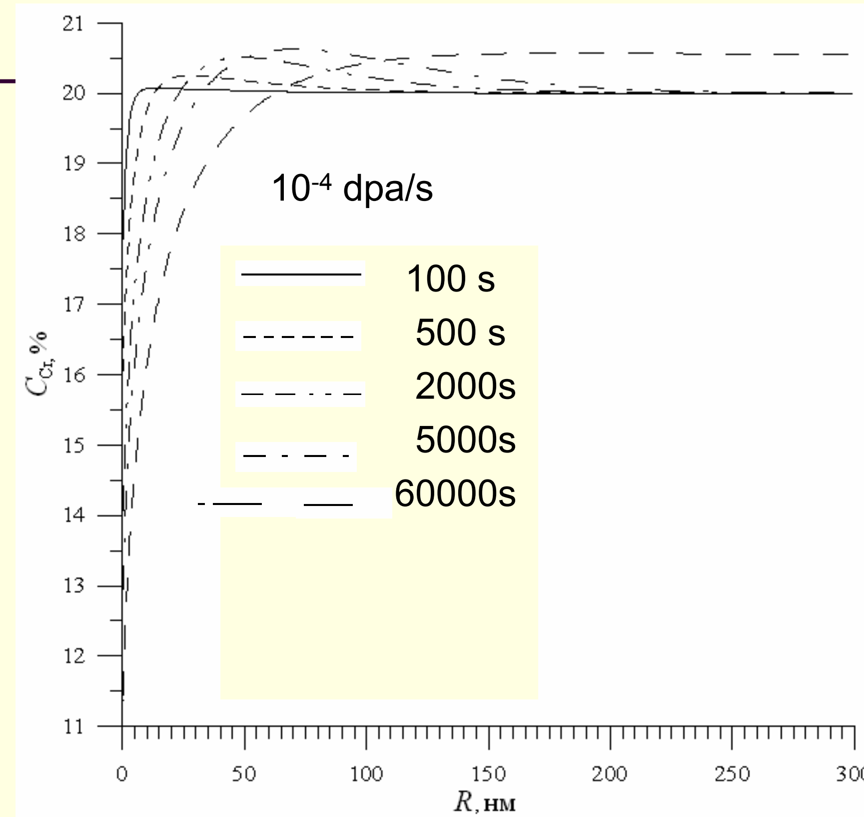

Calculated Cr profile developments near a sample surface of Fe-20Cr-12Ni alloy irradiated with 3 MeV Ni ions at a damage rates of 2×10^{-3} dpa/s and 10^{-4} dpa/s to a doses up to 6 dpa

Effect of dose rate

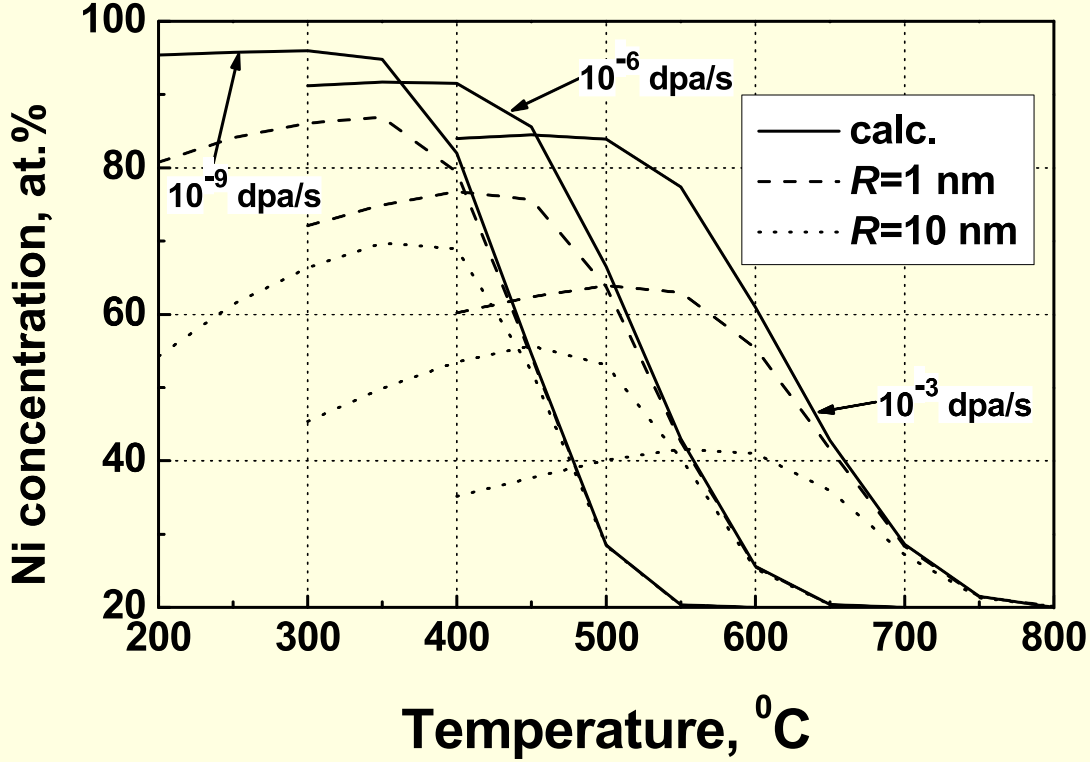

The temperature dependence of calculated and averaged Ni concentrations on GB in Fe-15Cr-20Ni alloy at 100 dpa and different dose rates *(Stepanov, Pechenkin, 2004)*

Effects of dose rate and temperature

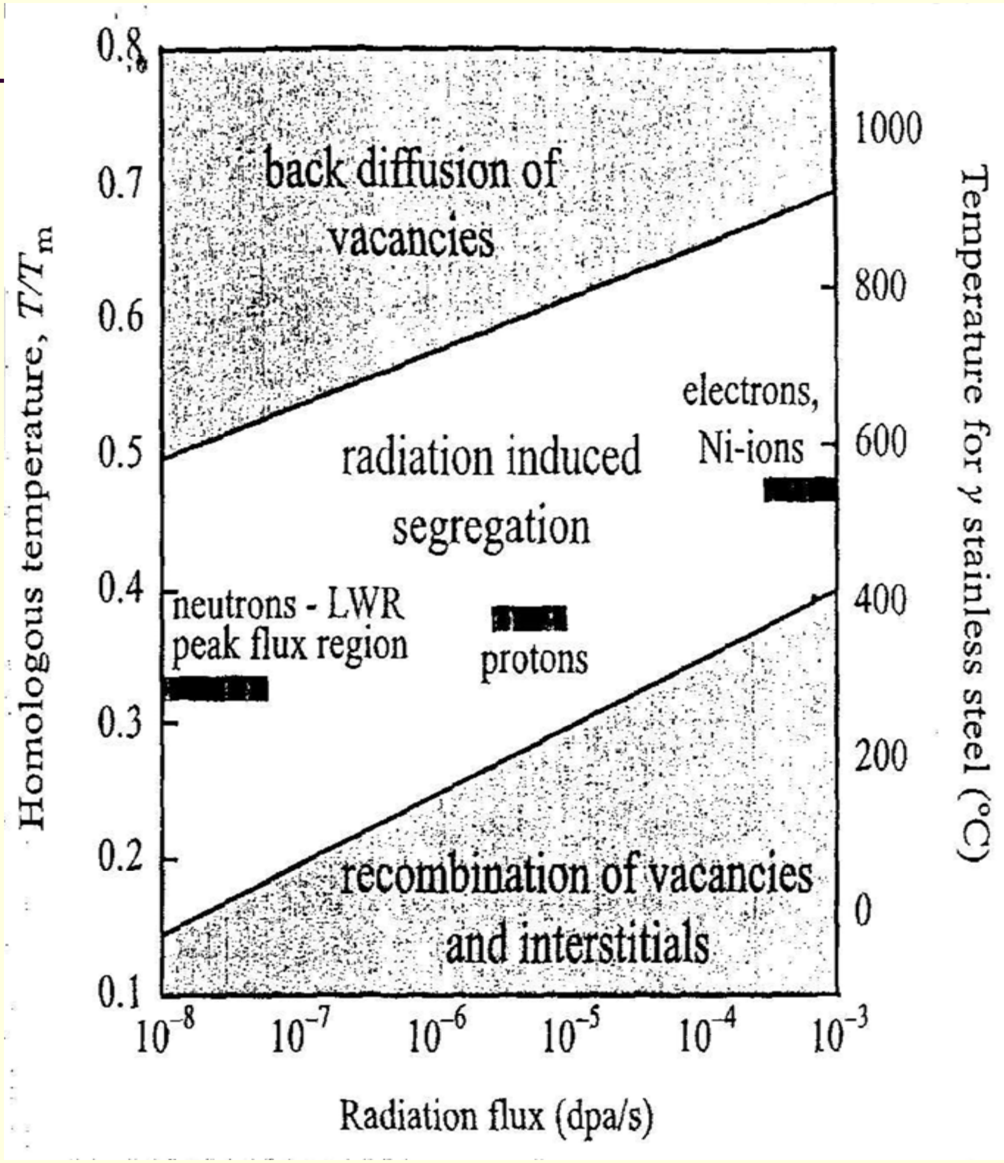

Relation between temperature and dose rate in the context of radiation-induced segregation, and the locations of neutron, proton and nickel ion irradiations

(from Was, 2007)

Effect of RIS on radiation phenomena

Phase transformations

Radiation-modified

Radiation-retarded

Radiation-induced precipitates

Austenitic steels:

γ' (Ni_3Si), G ($M_6Ni_{16}Si_7$), phosphides attached to PD sinks

γ' shells around voids in Fe-18Cr-8Ni-1Si and Nimonic Pe16

α-ferrit formation during FBR irradiation in initial γ–austenitic matrix near PD sinks (GB, voids, Ni-rich precipitates), which are in turn encased with Ni-rich austenite shells

Ferritic/martensitic steels:

α' , M_6C (increased content of Ni, Si, P) and G phases

Precipitate phases in irradiated 316 SS

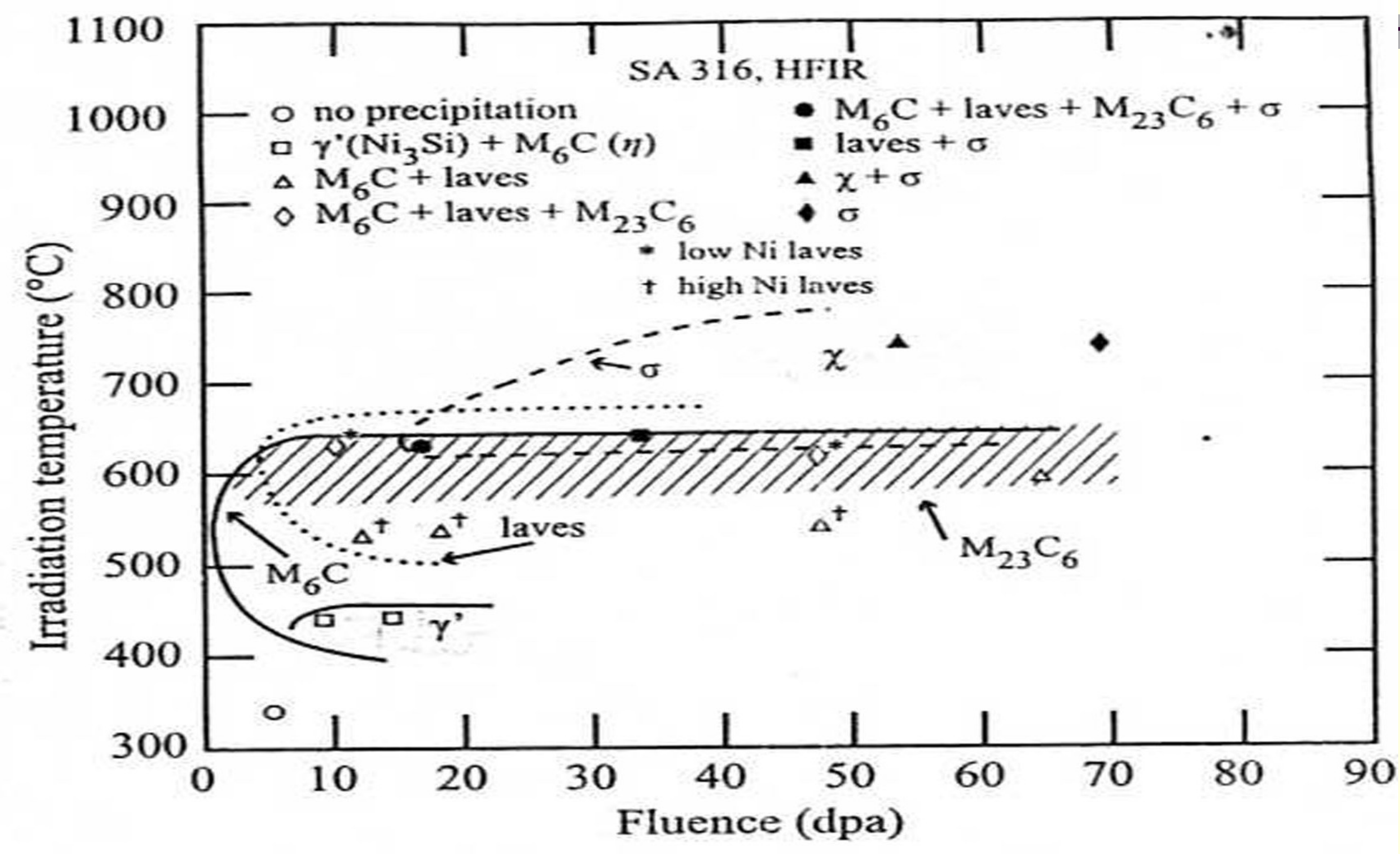

Dose and temperature dependence of precipitate phase formation in solution annealed 316 stainless steel irradiated in HFIR (from Was, 2007)

Radiation-induced precipitates

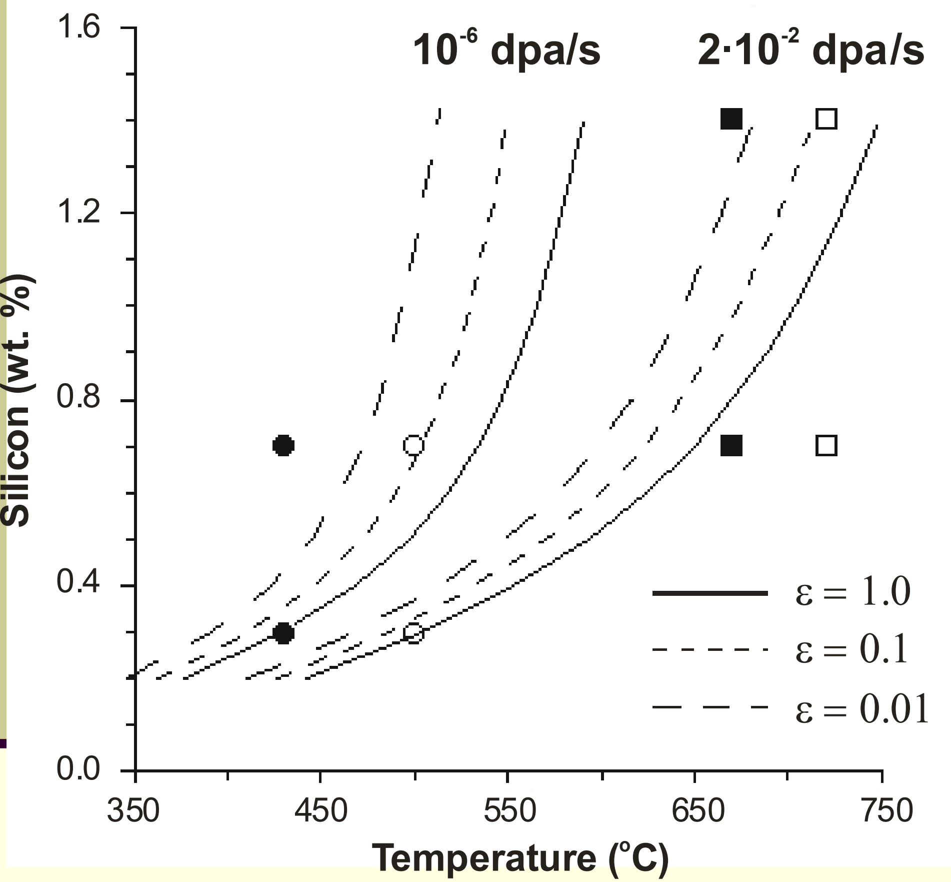

Calculated (Pechenkin et al., 1999) and observed (Garner et al., 1993) high-temperature boundary of γ′ precipitates stability in Fe-15Cr-20Ni-Si alloy irradiated with neutrons in the EBR-2 at 10^{-6} dpa/s (circles) and with 5 MeV Ni^{+} ions at 2×10^{-2} dpa/s (squares)

filled - observed

empty - not observed

A criterion is put in the basis of the treatment: a precipitate is unstable at temperatures, at which the concentration of a "crucial" component (Si here) near sinks set due to RIS is less than the corresponding solubility limit of the component for this precipitate

Radiation-induced precipitates

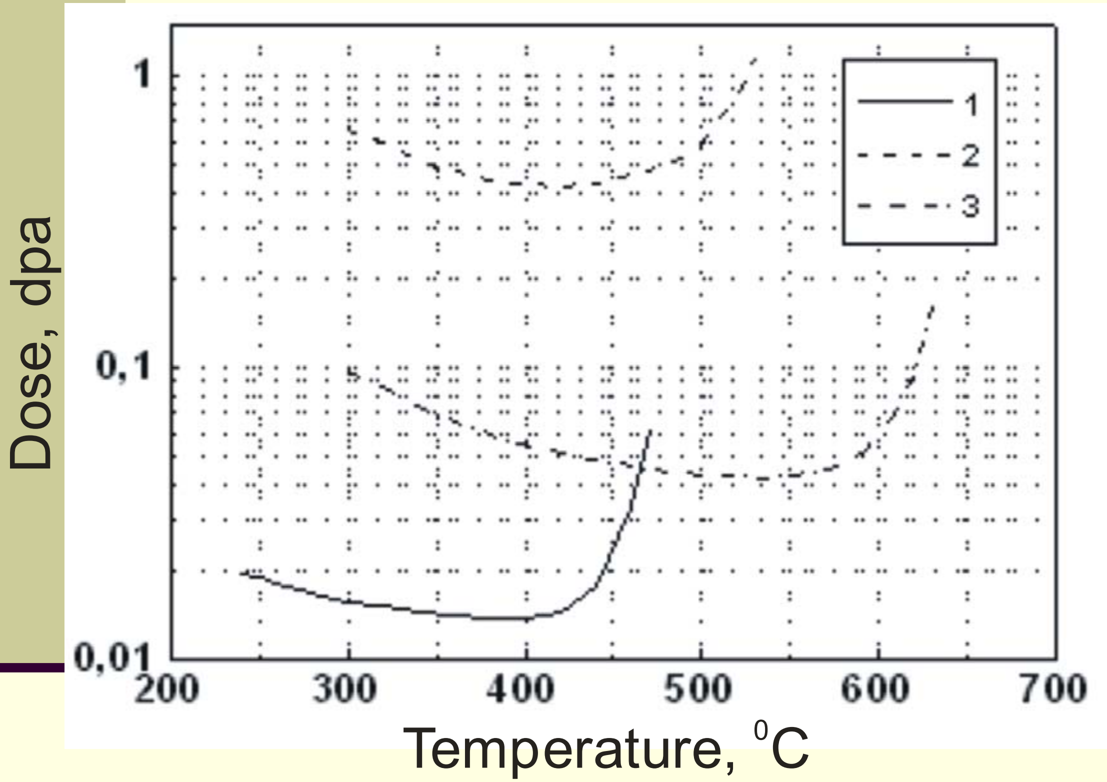

Calculation of dose-temperature stability regions for γ′ precipitates in X18H10T (Pechenkin, Stepanov, 1999)

Temperature dependence of incubation dose for γ' phase formation:

1) $K=10^{-6}$ dpa/s, $\varepsilon=0.1$, $E_{Si}^{b}=0.16$ eV, *2) $K=10^{-3}$ dpa/s, $\varepsilon=1$, $E_{Si}^{b}=0.16$ eV,*

3) $K=10^{-3}$ dpa/s, $\varepsilon=1$, $E_{Si}^{b}=0.23$ eV

Radiation-retarded precipitates

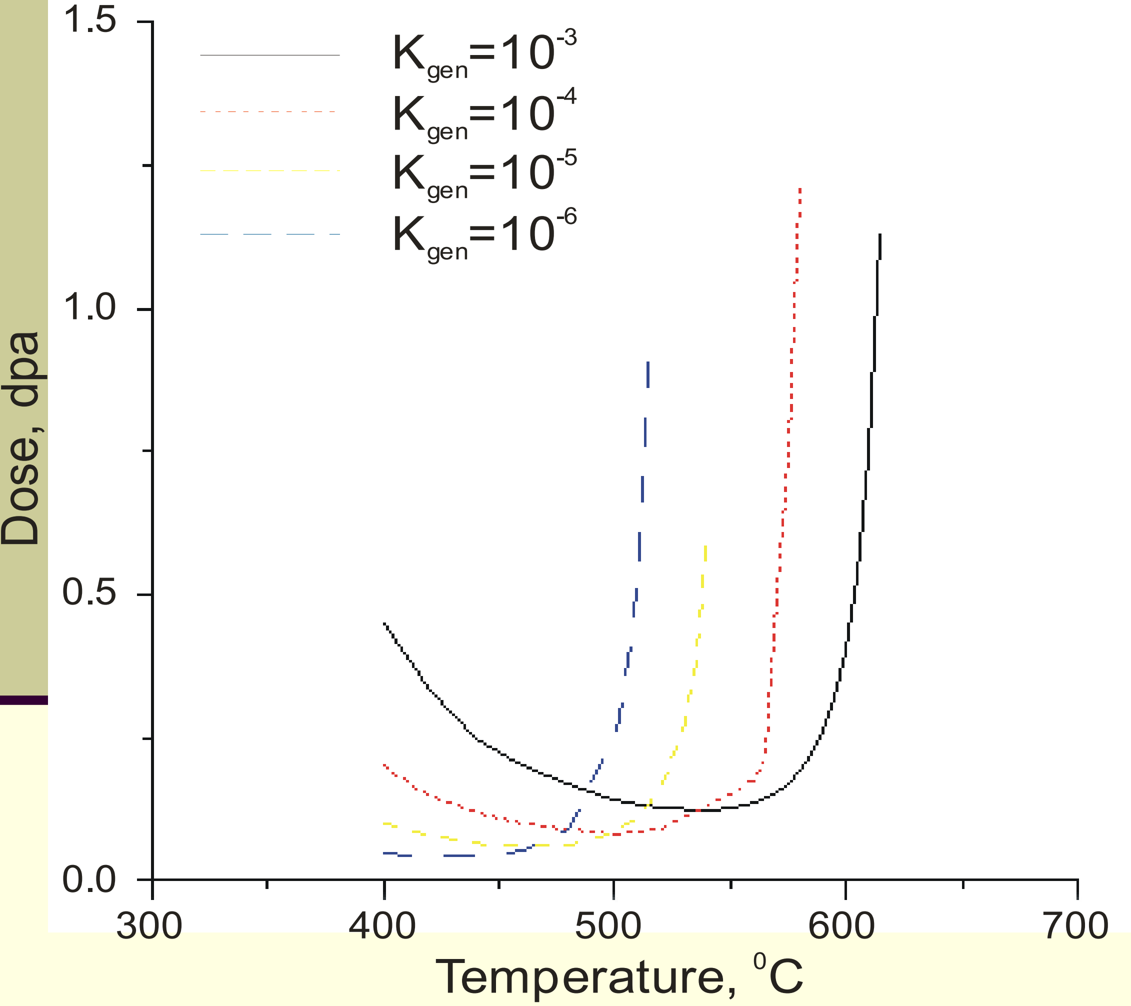

Calculation of dose-temperature stability regions for $M_{23}C_6$ precipitates on GB in AISI304 (Pechenkin, Stepanov, 1999)

Analytical model of radiation-induced precipitation at the surface of dilute binary alloy

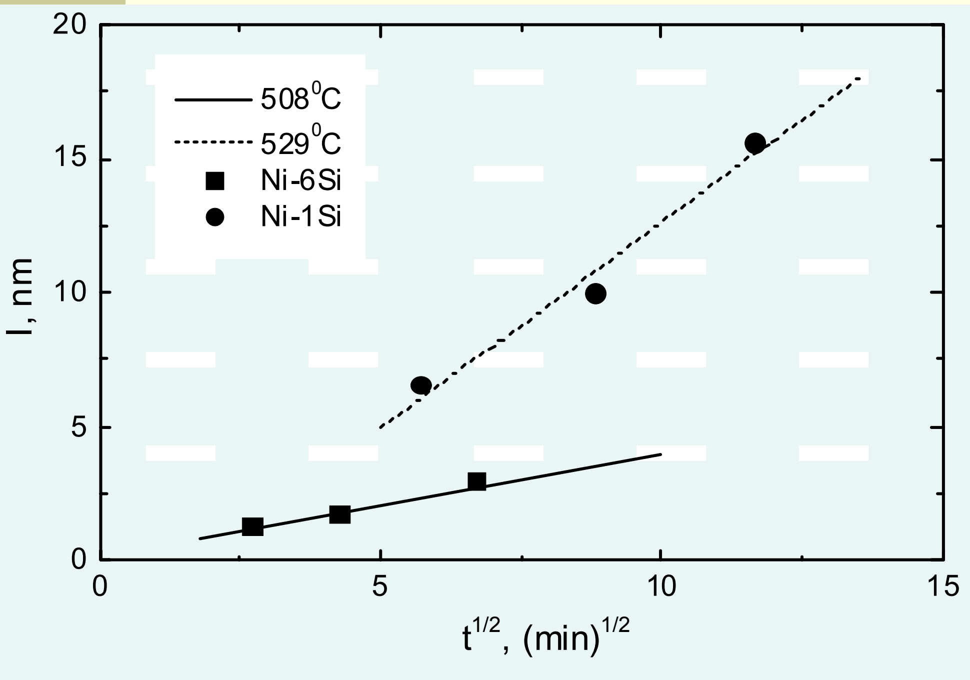

Growth curves for Ni_3Si films on Ni-Si alloys during irradiation with 3 MeV ions at a dose-rate of 6.9×10^{-4} dpa/s (Okamoto et. al, 1981)

Model of precipitate layer growth at the foil surface of an undersaturated binary alloy under irradiation is developed (Pechenkin et al., 2002).

A parabolic law of the layer growth predicted is in greement with experimental data on γ'-phase growth at the surface of Ni-Si dilute alloys under ion irradiation

Effect of RIS on radiation phenomena

Swelling

1. *Segregation-induced bias of PD sinks (Kirkendall effect)*
   Strong dependence of swelling in Fe–Cr–Ni alloys on Ni content
   Large swelling in V–Fe, V–Cr alloys

2. *Enchanced growth rate of voids attached to radiation-induced precipitates* (G – phase, phosphides) in austenitic steels and in Xastelloy X

See Pechenkin3 for details

Effect of RIS on radiation phenomena

Irradiation assisted stress corrosion cracking of austenitic steels can be related to radiation-induced depletion of grain boundaries in Cr

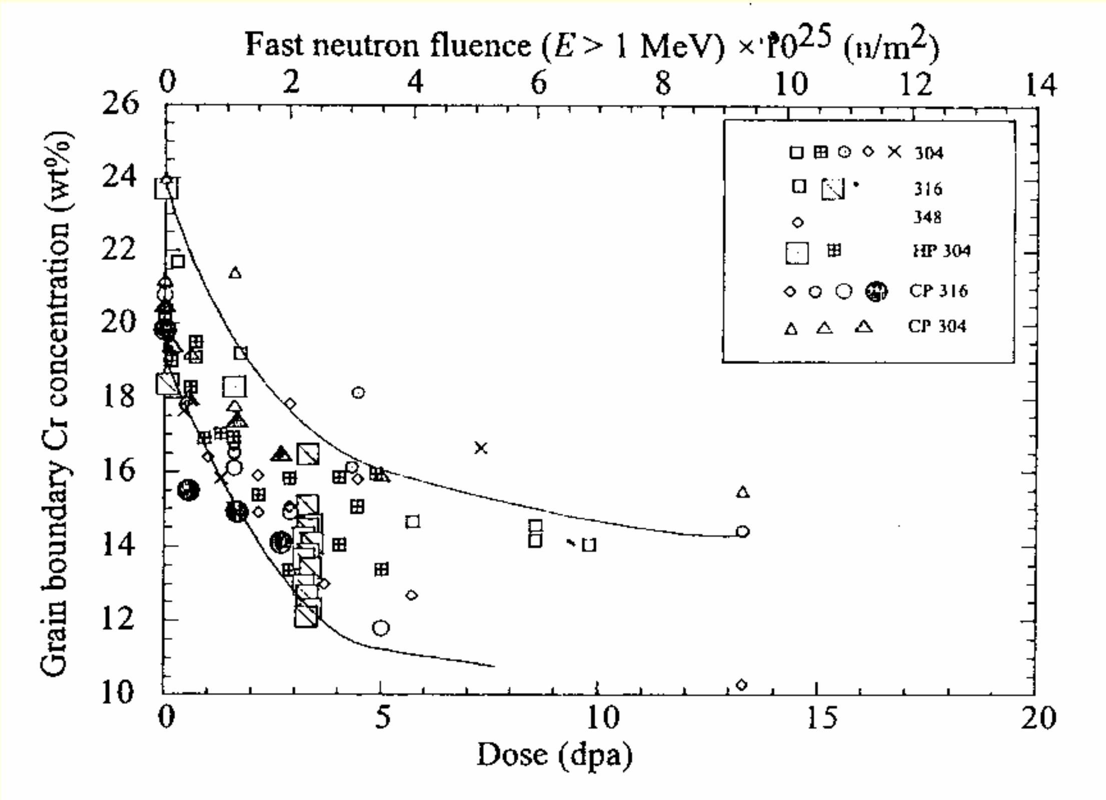

Effect of RIS on radiation phenomena

Radiation embrittlement of reactor pressure vessel steels

RIS of phosphorus at intergranular and interphase boundaries

Significant contribution of intergranular embrittlement at high neutron fluences

See Pechenkin2 for details

Experimental methods used and data needed

Experimental methods

Secondary ion mass spectroscopy (SIMS)

Scanning Auger microscopy (SAM)

Atom probe and field ion microscopy (APFIM)

Tomographic atom probe (TAP)

Field emission gun scanning transmission electron microscopy (FEGSTEM)

Most information on RIS near various PD sinks is obtained by the letter method

Data on component diffusivities via vacancy and interstitial mechanisms are needed for modeling RIS in alloys of interest

Ab initio calculations of PD formation and migration energies in alloys

Molecular dynamics calculations of alloy component diffusivities with reliable potentials fitted to experimental data and ab initio calculations

Conclusions

- Radiation induced segregation (RIS) effects essentially on precipitation, swelling, irradiation-assisted stress corrosion cracking and embrittlement of alloys. The higher the propensity of an alloy to RIS the more considerable properties alteration it can reveal
- A necessary stage of new radiation-resistant alloys development should be a preliminary investigation of RIS phenomenon and radiation-induced formation of precipitates in express irradiation experiments.
- The irradiation of alloys with heavy ions of MeV-energy in a wide range of temperatures and doses seems as appropriate method of such investigations.